

# GOWDY PHENOMENOLOGY IN SCALE-INVARIANT VARIABLES

LARS ANDERSSON<sup>1</sup>, HENK VAN ELST, AND CLAES UGGLA<sup>2</sup>

ABSTRACT. The dynamics of Gowdy vacuum spacetimes is considered in terms of Hubble-normalized scale-invariant variables, using the timelike area temporal gauge. The resulting state space formulation provides for a simple mechanism for the formation of “false” and “true spikes” in the approach to the singularity, and a geometrical formulation for the local attractor.

## 1. INTRODUCTION

Our map of general relativity has been, and still is, full of areas marked “Terra Incognita”. Its oceans and forests are as full of monsters, as ever the outer limits of the world during the dark ages. Only recently hunters have gone out to bring down some of the large prey of general relativity. This is a hunt that requires the utmost ingenuity and perseverance of the hunter. It is with pleasure that we dedicate this paper to Vince Moncrief, who has brought home a number of prize specimens, both in the field of general relativity as well as on the African veldt.

The cosmic censorship conjecture is the most elusive of the game animals of general relativity. No one has come close to bringing it down, though it is the subject of many stories told around the camp fires. However, some of its lesser cousins, appearing as cosmologies with isometries, can and have been hunted successfully. Here, Vince Moncrief has consistently led the way. This is true for spatially homogeneous (Bianchi) cosmologies, Gowdy vacuum spacetimes, as well as  $U(1)$ -symmetric spacetimes. In addition, he has made fundamental contributions to our understanding of the structure of 3+1 dimensional spacetimes with no isometries.

In this paper we will discuss Gowdy vacuum spacetimes, a class of spatially inhomogeneous cosmological models with no matter sources, two commuting spacelike Killing vector fields, and compact spacelike sections. Gowdy spacetimes are named after Robert H. Gowdy who, inspired by a study of Einstein-Rosen gravitational wave metrics [16]<sup>1</sup>, initially investigated this class of metrics [22, 23]. The dynamics of Gowdy spacetimes exhibit considerable

---

*Date:* October 29, 2003.

*To appear in:* A Spacetime Safari: Papers in Honour of Vincent Moncrief.

<sup>1</sup>Supported in part by the Swedish Research Council, contract no. R-RA 4873-307 and the NSF, contract no. DMS 0104402.

<sup>2</sup>Supported by the Swedish Research Council.

<sup>1</sup>Piotr Chruściel pointed out that Einstein-Rosen metrics were discussed more than a decade earlier by Guido Beck [1, §2].

complexity, and reflect the nonlinear interactions between the two polarization states of gravitational waves. The symmetry assumption restricts the spatial topology to  $\mathbf{S}^3$ ,  $\mathbf{S}^1 \times \mathbf{S}^2$ , or  $\mathbf{T}^3$ . In a series of papers, Moncrief and collaborators have built up a picture of the large scale structure of these spacetimes, and, in particular, of the nature of their cosmological singularities.

In Ref. [33], Vince Moncrief laid the foundation for the analysis of Gowdy vacuum spacetimes, by providing a Hamiltonian framework and proving, away from the singularity, the global existence of smooth solutions to the associated initial value problem. The Hamiltonian formulation has played a central rôle in the later work with Berger; in particular, in the method of consistent potentials (see Refs. [4] and [6] for a discussion).

Isenberg and Moncrief [28] proved that for polarized Gowdy vacuum spacetimes (i) the approach to the singularity is “asymptotically velocity-term dominated” (AVTD), i.e., the asymptotic dynamics is Kasner-like, and (ii) in general the spacetime curvature becomes unbounded. Chruściel *et al* [11] constructed polarized Gowdy vacuum spacetimes with prescribed regularity at the singularity, while Isenberg *et al* [27] studied the evolution towards the singularity of the Bel–Robinson energy in the unpolarized case.

Grubišić and Moncrief [24] studied perturbative expansions of solutions for Gowdy vacuum spacetimes with topology  $\mathbf{T}^3 \times \mathbf{R}$  near the singularity, which are consistent when a certain “low velocity” assumption holds. Based on the intuition developed in this work, Kichenassamy and Rendall [29] used the Fuchsian algorithm to construct whole families of solutions, depending on the maximum possible number of four (here analytic) free functions.

Berger and Moncrief [8] performed numerical simulations of the approach to the singularity and found that “spiky features” form in the solutions near the singularity, and that these features “freeze in”. A nongeneric condition used in the work of Grubišić and Moncrief [24] turns out to be related to the formation of spikes. Further numerical experiments clarifying the nature of the spiky features have been carried out by Berger and Garfinkle [5], and recently by Garfinkle and Weaver [21]. Garfinkle and Weaver studied the dynamical behavior of general spikes with “high velocity” in Gowdy vacuum spacetimes with topology  $\mathbf{T}^3 \times \mathbf{R}$ , using a combination of a Cauchy and a characteristic integration code. They found numerical evidence of a mechanism that drives spikes with initially “high velocity” to “low velocity” so that only spikes of the latter type appear to persist in the approach to the singularity.

The understanding of the spiky features for generic Gowdy vacuum spacetimes is the main obstacle to a complete understanding of the nature of the singularity in this setting. Rendall and Weaver [34] have constructed families of Gowdy vacuum spacetimes with spikes by an explicit transformation, starting from smooth “low velocity” solutions. In addition, they introduced a classification of spikes into “false spikes” (also: “downward pointing spikes”) and “true spikes” (also: “upward pointing spikes”), which by now has become part of the standard terminology in this area. Substantial progress in understanding the structure of Gowdy vacuum spacetimes going beyond what is possible by means of the Fuchsian algorithm has been made recently by Chae and Chruściel [9] and Ringström [36, 37].

In spite of the fact that Hamiltonian methods are Vince’s weapon of choice, in this paper we will bring the dynamical systems formalism, developed by John Wainwright, Claes Uggla and collaborators, to bear on the problem of understanding the dynamics of Gowdy vacuum spacetimes near the singularity (assuming spatial topology  $\mathbf{T}^3$  throughout). This approach is a complementary alternative to the method of consistent potentials, often used in the work of Moncrief, Berger and collaborators. The dynamical systems formalism breaks the canonical nature of the evolution equations by passing to a system of equations for typically Hubble-normalized scale-invariant orthonormal frame variables. The picture of a dynamical state space with a hierarchical structure emerges naturally. By casting the evolution equations into a first order form, this approach allows one to extract an asymptotic dynamical system which approximates the dynamics near the singularity increasingly accurately. The guiding principle for understanding the approach to the singularity is “asymptotic silence”, the gradual freezing-in of the propagation of geometrical information due to rapidly increasing spacetime curvature. One finds that in this regime, with spacetime curvature radii of the order of the Planck scale, the dynamics along individual timelines can be approximated by the asymptotic dynamics of spatially self-similar and spatially homogeneous models — a feature directly associated with the approach to the so-called “silent boundary.”

**1.1. Dynamical systems methods.** In this paper, we will study Gowdy vacuum spacetimes in terms of Hubble-normalized scale-invariant orthonormal frame variables. This approach was first pursued systematically in the context of spatially homogeneous (Bianchi) cosmology by Wainwright and Hsu [41]<sup>2</sup>, building on earlier work by Collins [12]. The main reference on this material is the book edited by Wainwright and Ellis (WE) [40], where techniques from the theory of dynamical systems are applied to study the asymptotic dynamics of cosmological models with a perfect fluid matter source that have isometries.

Hewitt and Wainwright [26] obtained a Hubble-normalized system of equations for spatially inhomogeneous cosmological models with a perfect fluid matter source that admit an Abelian  $G_2$  isometry group which acts orthogonally transitively (i.e., there exists a family of timelike 2-surfaces orthogonal to the  $G_2$ -orbits).<sup>3</sup> When restricting these models to the vacuum subcase, imposing topology  $\mathbf{T}^2$  on the  $G_2$ -orbits, and compactifying the coordinate associated with the spatial inhomogeneity (so that overall spatial topology  $\mathbf{T}^3$  results), one gets Gowdy vacuum spacetimes as an invariant set.

The nature of the singularity in orthogonally transitive perfect fluid  $G_2$  cosmologies has been studied by dynamical systems methods in Ref. [20], where the area expansion rate of the  $G_2$ -orbits was used as a normalization variable instead of the more common Hubble scalar  $H$ . In recent work, Uggla *et al* [38] introduced a general dynamical systems framework for dealing with perfect fluid  $G_0$  cosmologies, i.e., the full 3+1 dimensional case without isometries.

---

<sup>2</sup>More accurately, in this work the authors employed the volume expansion rate  $\Theta$  as the normalization variable rather than the Hubble scalar  $H$ ; these two variables are related by  $\Theta = 3H$ .

<sup>3</sup>See previous footnote.

Using again a Hubble-normalized system of equations, this work studies the asymptotic dynamics of the approach to the singularity. Physical considerations suggest that the past directed evolution gradually approaches a boundary of the  $G_0$  state space on which the Hubble-normalized frame variables  $E_\alpha^i$ , i.e., the coefficients of the spatial derivatives, vanish. This so-called “silent boundary” is distinguished by a reduction of the evolution equations to an effective system of ordinary differential equations, with position dependent coefficients. In this dynamical regime, typical orbits in the  $G_0$  state space shadow more and more closely the subset of orbits in the silent boundary, governed by the scale-invariant evolution equations restricted to the silent boundary, which coincide with the evolution equations for spatially self-similar and spatially homogeneous models. It is a strength of the dynamical systems framework that it provides for the possibilities (i) to make some interesting conjectures on the nature of the local past attractor for the Hubble-normalized system of equations of  $G_0$  cosmology, and, in particular, (ii) to give a precise mathematical formulation of the well known BKL<sup>4</sup> conjecture in theoretical cosmology: For almost all cosmological solutions of Einstein’s field equations, a spacelike initial singularity is silent, vacuum dominated and oscillatory (see Refs. [2, §§2,3], [3, §§3,5] and [38, §6]). Both the AVTD behavior of Gowdy vacuum spacetimes and the past attractor associated with the BKL conjecture turn out to be associated with invariant subsets on the silent boundary. Moreover, the dynamics on the silent boundary also governs the *approach* towards these subsets. Hence, the silent boundary provides a natural setting for studying AVTD as well as asymptotic oscillatory BKL behavior, and how such behavior arises.

**1.2. Overview of this paper.** In Sec. 2, we introduce the system of equations for Gowdy vacuum spacetimes with topology  $\mathbf{T}^3 \times \mathbf{R}$  in the metric form used in the work of Moncrief and collaborators, and also describe the orthonormal frame variables. In Sec. 3, we introduce two alternative scale-invariant systems of equations. In Subsec. 3.1, we introduce Hubble-normalized variables, and derive the system of evolution equations and constraints which govern the dynamics of the Hubble-normalized state vector  $\mathbf{X}(t, x)$ . In Subsec. 3.2, on the other hand, we discuss the area expansion rate-normalized variables and equations, introduced in Ref. [20]. Invariant sets of the Hubble-normalized system of equations for Gowdy vacuum spacetimes are described in Sec. 4, the most notable ones being the polarized models and the silent boundary of the Hubble-normalized state space; the latter is associated with spatially self-similar and spatially homogeneous models (including the Kasner subset). In Sec. 5, we start the discussion of the asymptotic dynamics towards the singularity of the Gowdy equations. In Subsec. 5.1, we review the picture found numerically by Moncrief, Berger and collaborators, and in Subsec. 5.2, we describe the phenomenology in terms of Hubble-normalized variables, using principles introduced in Refs. [38] and [20]. In particular, we numerically show that there is good agreement between state space orbits of the full Gowdy equations for  $\mathbf{X}(t, x)$  and state space orbits of the system of equations on the silent boundary. We thus give evidence for the hypothesis that the silent boundary describes both the final state and

---

<sup>4</sup>Named after Vladimir Belinskiĭ, Isaac Khalatnikov and Evgeny Lifshitz.

the approach towards it, as claimed above. We then derive and solve the system of ordinary differential equations which governs the asymptotic behavior of the state vector  $\mathbf{X}(t, x)$  in a neighborhood of the Kasner subset on the silent boundary. The connection between these analytic results and others obtained through various numerical experiments are subsequently discussed. In particular, we point out the close correspondence between the formation of spikes and state space orbits of  $\mathbf{X}(t, x)$  of Bianchi Type-I and Type-II, for timelines  $x = \text{constant}$  close to spike point timelines. In Subsec. 5.3, we then comment on the behavior of the Hubble-normalized Weyl curvature in the “low velocity” regime. In Sec. 6, we conclude with some general remarks. We discuss the dynamical nature of the silent boundary of the state space, relate this concept to the AVTD and BKL pictures in Subsec. 6.1, and review its application to Gowdy vacuum spacetimes in Subsec. 6.2. We also comment on the conjectural picture that emerges from the present work, and make links to a more general context. Finally, expressions for the Hubble-normalized components of the Weyl curvature tensor, as well as some scalar quantities constructed from it, are given in an appendix.

## 2. GOWDY VACUUM SPACETIMES

**2.1. Metric approach.** Gowdy vacuum spacetimes with topology  $\mathbf{T}^3 \times \mathbf{R}$  are described by the metric<sup>5</sup> (in units such that  $c = 1$ , and with  $\ell_0$  the unit of the physical dimension [length])

$$\begin{aligned} \ell_0^{-2} ds^2 = & e^{(t-\lambda)/2} (-e^{-2t} dt^2 + dx^2) \\ & + e^{-t} [e^P (dy_1 + Q dy_2)^2 + e^{-P} dy_2^2] , \end{aligned} \quad (2.1)$$

using the sign conventions of Berger and Garfinkle [5], but denoting by  $t$  their time coordinate  $\tau$ . The metric variables  $\lambda$ ,  $P$  and  $Q$  are functions of the local coordinates  $t$  and  $x$  only. Each of the spatial coordinates  $x$ ,  $y_1$  and  $y_2$  has period  $2\pi$ , while the (logarithmic) area time coordinate  $t$  runs from  $-\infty$  to  $+\infty$ , with the singularity at  $t = +\infty$ . This metric is invariant under the transformations generated by an Abelian  $G_2$  isometry group, with spacelike Killing vector fields  $\xi = \partial_{y_1}$  and  $\eta = \partial_{y_2}$  acting orthogonally transitively on  $\mathbf{T}^2$  (see, e.g., Hewitt and Wainwright [26]). Note that the volume element on  $\mathbf{T}^3$  is given by  $\sqrt{{}^3g} = \ell_0^3 e^{-(3t+\lambda)/4}$ .

Einstein’s field equations in vacuum give for  $P$  and  $Q$  the coupled semilinear wave equations

$$P_{,tt} - e^{-2t} P_{,xx} = e^{2P} (Q_{,t}^2 - e^{-2t} Q_{,x}^2) , \quad (2.2a)$$

$$Q_{,tt} - e^{-2t} Q_{,xx} = -2 (P_{,t} Q_{,t} - e^{-2t} P_{,x} Q_{,x}) , \quad (2.2b)$$

and for  $\lambda$  the Gauß and Codacci constraints

$$0 = \lambda_{,t} - [P_{,t}^2 + e^{-2t} P_{,x}^2 + e^{2P} (Q_{,t}^2 + e^{-2t} Q_{,x}^2)] , \quad (2.3a)$$

$$0 = \lambda_{,x} - 2 (P_{,t} P_{,x} + e^{2P} Q_{,t} Q_{,x}) . \quad (2.3b)$$

---

<sup>5</sup>The most general form of the Gowdy metric on  $\mathbf{T}^3 \times \mathbf{R}$  has been given in Ref. [10, §2]. However, the additional constants appearing in that paper have no effect on the evolution equations.

For Gowdy vacuum spacetimes the evolution (wave) equations decouple from the constraints. Consequently, the initial data for  $P$ ,  $Q$ ,  $P_{,t}$  and  $Q_{,t}$  as  $2\pi$ -periodic real-valued functions of  $x$  can be specified freely, subject only to appropriate requirements of minimal differentiability and the zero total linear momentum condition [33]

$$0 = \int_0^{2\pi} \lambda_{,x} dx . \quad (2.4)$$

The fact that the initial data contains four arbitrary functions supports the interpretation of Gowdy vacuum spacetimes as describing nonlinear interactions between the two polarization states of gravitational waves. The so-called polarized Gowdy vacuum spacetimes form the subset of solutions with  $0 = Q_{,t} = Q_{,x}$ . Note that in this case, without loss of generality, a coordinate transformation on  $\mathbf{H}^2$  can be used to set  $0 = Q$  identically, and thus obtain the standard diagonal form of the metric.

As is well known, the metric functions  $P$  and  $Q$  can be viewed as coordinates on the hyperbolic plane  $\mathbf{H}^2$  (this is just the Teichmüller space of the flat metrics on the  $\mathbf{T}^2$  orbits of the  $G_2$  isometry group), with metric

$$g_{\mathbf{H}^2} = dP^2 + e^{2P} dQ^2 . \quad (2.5)$$

The Gowdy evolution equations form a system of wave equations which is essentially a 1+1 dimensional wave map system with a friction term, the target space being  $\mathbf{H}^2$ . The sign of the friction term is such that the standard wave map energy decreases in the direction *away* from the singularity, i.e., as  $t \rightarrow -\infty$ . The friction term diverges as  $t \rightarrow +\infty$ . This is more easily seen using the dimensional time coordinate  $\tau = \ell_0 e^{-t}$ . In terms of this time coordinate, the wave equations take the form

$$-\partial_\tau^2 u - \frac{1}{\tau} \partial_\tau u + \partial_x^2 u + \Gamma(\partial u \cdot \partial u) = 0 , \quad (2.6)$$

where this can be seen explicitly. Here  $u$  is a map  $u: \mathbf{R}^{1,1} \rightarrow \mathbf{H}^2$ , and  $\Gamma$  are the Christoffel symbols defined with respect to the coordinates used on  $\mathbf{H}^2$ . It is convenient to define a hyperbolic velocity  $v$  by

$$v := \|\partial_t u\|_{\mathbf{H}^2} = \sqrt{P_{,t}^2 + e^{2P} Q_{,t}^2} . \quad (2.7)$$

Then  $v(t, x)$  is the velocity in  $(\mathbf{H}^2, g_{\mathbf{H}^2})$  of the point  $[P(t, x), Q(t, x)]$  (cf. Ref. [24]).

**2.2. Orthonormal frame approach.** In the orthonormal frame approach, Gowdy vacuum spacetimes arise as a subcase of vacuum spacetimes which admit an Abelian  $G_2$  isometry group that acts *orthogonally transitively* on spacelike 2-surfaces (cf. Refs. [26] and [20]). One introduces a group invariant orthonormal frame  $\{e_a\}_{a=0,1,2,3}$ , with  $e_0$  a vorticity-free timelike reference congruence,  $e_1$  a hypersurface-orthogonal vector field defining the direction of spatial inhomogeneity, and with  $e_2$  and  $e_3$  tangent to the  $G_2$ -orbits; the latter are generated by commuting spacelike Killing vector fields  $\xi$  and  $\eta$  (see Ref. [39, §3] for further details). It is a convenient choice of spatial gauge to globally align  $e_2$  with  $\xi$ . Thus, within a (3+1)-splitting picture that employs a set of symmetry adapted

local coordinates  $x^\mu = (t, x, y_1, y_2)$ , the frame vector fields  $e_a$  can be expressed by

$$e_0 = N^{-1} \partial_t, \quad e_1 = e_1^1 \partial_x, \quad e_2 = e_2^2 \partial_{y_1}, \quad e_3 = e_3^2 \partial_{y_1} + e_3^3 \partial_{y_2}, \quad (2.8)$$

where, for simplicity, the shift vector field  $N^i$  was set to zero.

For Gowdy vacuum spacetimes with topology  $\mathbf{T}^3 \times \mathbf{R}$ , the orthonormal frame equations (16), (17) and (33)–(44) given in Ref. [19] need to be specialized by setting  $(\alpha, \beta = 1, 2, 3)$

$$0 = e_2(f) = e_3(f), \quad (2.9a)$$

$$0 = \omega^\alpha = \sigma_{31} = \sigma_{12} = a^\alpha = n_{1\alpha} = n_{33} = \dot{u}_2 = \dot{u}_3 = \Omega_2 = \Omega_3, \quad (2.9b)$$

$$0 = \mu = p = q^\alpha = \pi_{\alpha\beta}, \quad (2.9c)$$

for  $f$  any spacetime scalar. The remaining nonzero connection variables are

- (1)  $\Theta$ , which measures the volume expansion rate of the integral curves of  $e_0$ ; it determines the *Hubble scalar*  $H$  by  $H := \frac{1}{3} \Theta$ ,
- (2)  $\sigma_{11}$ ,  $\sigma_{22}$ ,  $\sigma_{33}$  and  $\sigma_{23}$  (with  $0 = \sigma_{11} + \sigma_{22} + \sigma_{33}$ ), which measure the shear rate of the integral curves of  $e_0$ ,
- (3)  $n_{22}$  and  $n_{23}$ , which are commutation functions for  $e_1$ ,  $e_2$  and  $e_3$  and constitute the spatial connection on  $\mathbf{T}^3$ ,
- (4)  $\dot{u}_1$ , the acceleration (or nongeodesity) of the integral curves of  $e_0$ , and
- (5)  $\Omega_1$ , the angular velocity at which the frame vector fields  $e_2$  and  $e_3$  rotate about the Fermi propagated<sup>6</sup> frame vector field  $e_1$ .

The area density  $\mathcal{A}$  of the  $G_2$ -orbits is defined (up to a constant factor) by

$$\mathcal{A}^2 := (\xi_a \xi^a)(\eta_b \eta^b) - (\xi_a \eta^a)^2, \quad (2.10)$$

which, in terms of the coordinate components of the frame vector fields  $e_2$  and  $e_3$  tangent to the  $G_2$ -orbits, becomes

$$\mathcal{A}^{-1} = e_2^2 e_3^3. \quad (2.11)$$

The physical dimension of  $\mathcal{A}$  is [length]<sup>2</sup>. The key equations for  $\mathcal{A}$ , derivable from the commutators (16) and (17) in Ref. [19], are

$$N^{-1} \frac{\partial_t \mathcal{A}}{\mathcal{A}} = (2H - \sigma_{11}), \quad e_1^1 \frac{\partial_x \mathcal{A}}{\mathcal{A}} = 0, \quad (2.12)$$

i.e.,  $(2H - \sigma_{11})$  is the area expansion rate of the  $G_2$ -orbits.

We now introduce connection variables  $\sigma_+$ ,  $\sigma_-$ ,  $\sigma_\times$ ,  $n_-$  and  $n_\times$  by

$$\sigma_+ = \frac{1}{2}(\sigma_{22} + \sigma_{33}) = -\frac{1}{2}\sigma_{11}, \quad \sigma_- = \frac{1}{2\sqrt{3}}(\sigma_{22} - \sigma_{33}), \quad (2.13a)$$

$$\sigma_\times = \frac{1}{\sqrt{3}}\sigma_{23}, \quad n_- = \frac{1}{2\sqrt{3}}n_{22}, \quad (2.13b)$$

$$n_\times = \frac{1}{\sqrt{3}}n_{23}. \quad (2.13c)$$

Together with the Hubble scalar  $H$ , for Gowdy vacuum spacetimes this is a complete set of connection variables.

<sup>6</sup>A spatial frame vector field  $e_\alpha$  is said to be Fermi propagated along  $e_0$  if  $\langle e_\beta, \nabla_{e_0} e_\alpha \rangle = 0$ ,  $\alpha, \beta = 1, 2, 3$ .

Recall that  $\mathbf{e}_2$  was chosen such that it is globally aligned with  $\boldsymbol{\xi}$ . One finds that  $\Omega_1 = -\sqrt{3}\sigma_x$  (see Ref. [20, §3]). The spatial frame gauge variable  $\Omega_1$  quantifies the extent to which  $\mathbf{e}_2$  and  $\mathbf{e}_3$  are *not* Fermi propagated along  $\mathbf{e}_0$  in the dynamics of Gowdy vacuum spacetimes, starting from a given initial configuration.

We now give the explicit form of the natural orthonormal frame associated with the metric (2.1). With respect to the coordinate frame employed in Eq. (2.1), the frame vector fields are

$$\mathbf{e}_0 = N^{-1} \partial_t = \ell_0^{-1} e^{(3t+\lambda)/4} \partial_t, \quad (2.14a)$$

$$\mathbf{e}_1 = e_1^1 \partial_x = \ell_0^{-1} e^{-(t-\lambda)/4} \partial_x, \quad (2.14b)$$

$$\mathbf{e}_2 = e_2^2 \partial_{y_1} = \ell_0^{-1} e^{(t-P)/2} \partial_{y_1}, \quad (2.14c)$$

$$\mathbf{e}_3 = e_3^2 \partial_{y_1} + e_3^3 \partial_{y_2} = \ell_0^{-1} e^{(t+P)/2} (-Q \partial_{y_1} + \partial_{y_2}). \quad (2.14d)$$

Note that the lapse function is related to the volume element on  $\mathbf{T}^3$  by  $N = \ell_0^{-2} \sqrt{^3g}$ . Hence, in addition to being an area time coordinate,  $t$  is simultaneously a wavelike time coordinate.<sup>7</sup>

### 3. SCALE-INVARIANT VARIABLES AND EQUATIONS

**3.1. Hubble-normalization.** Following WE and Ref. [38], we now employ the Hubble scalar  $H$  as normalization variable to derive scale-invariant variables and equations to formulate the dynamics of Gowdy vacuum spacetimes with topology  $\mathbf{T}^3 \times \mathbf{R}$ . Hubble-normalized frame and connection variables are thus defined by

$$(\mathcal{N}^{-1}, E_1^1) := (N^{-1}, e_1^1)/H \quad (3.1)$$

$$(\Sigma_{\dots}, N_{\dots}, \dot{U}, R) := (\sigma_{\dots}, n_{\dots}, \dot{u}_1, \Omega_1)/H. \quad (3.2)$$

In order to write the dimensional equations<sup>8</sup> in dimensionless Hubble-normalized form, it is advantageous to introduce the deceleration parameter,  $q$  (which is a standard scale-invariant quantity in observational cosmology), and the logarithmic spatial Hubble gradient,  $r$ , by

$$(q+1) := -\mathcal{N}^{-1} \partial_t \ln(\ell_0 H), \quad (3.3)$$

$$r := -E_1^1 \partial_x \ln(\ell_0 H). \quad (3.4)$$

These two relations need to satisfy the integrability condition

$$\mathcal{N}^{-1} \partial_t r - E_1^1 \partial_x q = (q + 2\Sigma_+) r - (r - \dot{U})(q+1), \quad (3.5)$$

<sup>7</sup>By definition, wavelike time coordinates satisfy the equation  $g^{\mu\nu} \nabla_\mu \nabla_\nu t = f(x^\mu)$ ;  $f$  is a freely prescribable coordinate gauge source function of physical dimension  $[\text{length}]^{-2}$ . In terms of the lapse function, this equation reads  $N^{-1}(\partial_t - N^i \partial_i)N = 3HN + fN^2$ . For the metric (2.1) we have  $N^i = 0$  and  $f = 0$ ; the lapse equation thus integrates to  $N \propto \sqrt{^3g}$ . In the literature, wavelike time coordinates are often referred to as ‘‘harmonic time coordinates’’.

<sup>8</sup>In the orthonormal frame formalism, using units such that  $G/c^2 = 1 = c$ , the dynamical relations provided by the commutator equations, Einstein’s field equations and Jacobi’s identities all carry physical dimension  $[\text{length}]^{-2}$ .



as follows from the commutator equations (see Ref. [38] for the analogous  $G_0$  case). The Hubble-normalized versions of the key equations (2.12) are

$$\mathcal{N}^{-1} \frac{\partial_t \mathcal{A}}{\mathcal{A}} = 2(1 + \Sigma_+) , \quad E_1^1 \frac{\partial_x \mathcal{A}}{\mathcal{A}} = 0 , \quad (3.6)$$

so that the magnitude of the spacetime gradient  $\nabla_a \mathcal{A}$  is

$$(\nabla_a \mathcal{A})(\nabla^a \mathcal{A}) = -4H^2 (1 + \Sigma_+)^2 \mathcal{A}^2 . \quad (3.7)$$

Thus,  $\nabla_a \mathcal{A}$  is timelike as long as  $(1 + \Sigma_+)^2 > 0$ . As discussed later,  $\Sigma_+ = -1$  yields the (locally) Minkowski solution.

In terms of the Hubble-normalized variables, the hyperbolic velocity, defined in Eq. (2.7), reads

$$v = \sqrt{3} \frac{\sqrt{\Sigma_-^2 + \Sigma_\times^2}}{(1 + \Sigma_+)} ; \quad (3.8)$$

hence, it constitutes a scale-invariant measure of the transverse (with respect to  $e_1$ ) shear rate of the integral curves of  $e_0$ .

**3.1.1. Gauge choices.** The natural choice of temporal gauge is the *timelike area gauge* (see Ref. [20, §3] for terminology). In terms of the Hubble-normalized variables, this is given by setting

$$\mathcal{N} = \frac{C}{(1 + \Sigma_+)} , \quad C \in \mathbf{R} \setminus \{0\} , \quad (3.9)$$

$N^i = 0$ , so that by Eqs. (3.6) we have

$$\mathcal{A} = \ell_0^2 e^{2Ct} , \quad (3.10)$$

implying  $e_0 \parallel \nabla_a \mathcal{A}$ . This choice for  $\mathcal{N}$  and  $N^i$  thus defines the dimensionless (logarithmic) *area time coordinate*  $t$ . For convenience we keep the real-valued constant  $C$ , so that the direction of  $t$  can be reversed when this is preferred. With the choice  $C = -\frac{1}{2}$ ,  $t$  coincides with that used in the metric (2.1).

Having adopted a spatial gauge that globally aligns  $e_2$  with  $\xi$  has the consequence (see Ref. [20, §3])

$$R = -\sqrt{3}\Sigma_\times . \quad (3.11)$$

This fixes the value of the Hubble-normalized angular velocity at which  $e_2$  and  $e_3$  rotate about  $e_1$  during the evolution. Thus, while in this spatial gauge  $e_1$  is Fermi propagated along  $e_0$ ,  $e_2$  and  $e_3$  are *not*.

**3.1.2. Hubble-normalized equations.** The autonomous Hubble-normalized *constraints* are

$$(r - \dot{U}) = E_1^1 \partial_x \ln(1 + \Sigma_+) , \quad (3.12a)$$

$$1 = \Sigma_+^2 + \Sigma_-^2 + \Sigma_\times^2 + N_\times^2 + N_-^2 , \quad (3.12b)$$

$$(1 + \Sigma_+) \dot{U} = -3(N_\times \Sigma_- - N_- \Sigma_\times) . \quad (3.12c)$$

These follow, respectively, from the commutators and the Gauß and the Codacci constraints. The first is a gauge constraint, induced by fixing  $\mathcal{N}$  according to Eq. (3.9). Note that Eq. (3.12b) bounds the magnitudes of the Hubble-normalized variables  $\Sigma_+$ ,  $\Sigma_-$ ,  $\Sigma_\times$ ,  $N_\times$  and  $N_-$  between the values 0 and 1.

The autonomous Hubble-normalized *evolution equations* are

$$C^{-1}(1 + \Sigma_+) \partial_t E_1^1 = (q + 2\Sigma_+) E_1^1, \quad (3.13a)$$

$$C^{-1}(1 + \Sigma_+) \partial_t(1 + \Sigma_+) = (q - 2)(1 + \Sigma_+), \quad (3.13b)$$

$$\begin{aligned} C^{-1}(1 + \Sigma_+) \partial_t \Sigma_- + E_1^1 \partial_x N_\times &= (q - 2) \Sigma_- + (r - \dot{U}) N_\times \\ &\quad + 2\sqrt{3} \Sigma_\times^2 - 2\sqrt{3} N_-^2, \end{aligned} \quad (3.13c)$$

$$C^{-1}(1 + \Sigma_+) \partial_t N_\times + E_1^1 \partial_x \Sigma_- = (q + 2\Sigma_+) N_\times + (r - \dot{U}) \Sigma_-, \quad (3.13d)$$

$$\begin{aligned} C^{-1}(1 + \Sigma_+) \partial_t \Sigma_\times - E_1^1 \partial_x N_- &= (q - 2 - 2\sqrt{3} \Sigma_-) \Sigma_\times \\ &\quad - (r - \dot{U} + 2\sqrt{3} N_\times) N_-, \end{aligned} \quad (3.13e)$$

$$\begin{aligned} C^{-1}(1 + \Sigma_+) \partial_t N_- - E_1^1 \partial_x \Sigma_\times &= (q + 2\Sigma_+ + 2\sqrt{3} \Sigma_-) N_- \\ &\quad - (r - \dot{U} - 2\sqrt{3} N_\times) \Sigma_\times, \end{aligned} \quad (3.13f)$$

where

$$q = 2(\Sigma_+^2 + \Sigma_-^2 + \Sigma_\times^2) - \frac{1}{3}(E_1^1 \partial_x - r + \dot{U}) \dot{U}. \quad (3.14)$$

Note that from Eq. (3.13b)  $q$  can also be expressed by

$$q = 2 + C^{-1} \partial_t(1 + \Sigma_+). \quad (3.15)$$

Equations (3.12)–(3.14) govern the dynamics on the Hubble-normalized state space for Gowdy vacuum spacetimes of the state vector

$$\mathbf{X} = (E_1^1, \Sigma_+, \Sigma_-, N_\times, \Sigma_\times, N_-)^T. \quad (3.16)$$

Initial data can be set freely, as suitably differentiable  $2\pi$ -periodic real-valued functions of  $x$ , for the four variables  $\Sigma_-$ ,  $N_\times$ ,  $\Sigma_\times$  and  $N_-$ . Up to a sign, the data for  $\Sigma_+$  then follows from the Gauß constraint (3.12b), while the data for  $\dot{U}$  follows from the Codacci constraint (3.12c). The data for  $r$ , finally, is obtained from the gauge constraint (3.12a). Note that there is no free function associated with  $E_1^1$ . Any such function can be absorbed in a reparametrization of the coordinate  $x$ .

It is generally helpful to think of the variable pair  $(\Sigma_-, N_\times)$  as relating to the “+–polarization state” and the variable pair  $(\Sigma_\times, N_-)$  as relating to the “×–polarization state” of the gravitational waves in Gowdy vacuum spacetimes (see also Ref. [20, p. 58]).

**3.1.3. Conversion formulae.** We will now express the Hubble-normalized frame and connection variables in terms of the metric variables  $\lambda$ ,  $P$  and  $Q$ . For the metric (2.1), the choice for the nonzero real-valued constant  $C$  is

$$C = -\frac{1}{2}.$$

The Hubble scalar, given by  $H = \frac{1}{3} N^{-1} (\partial_t \sqrt{3g}) / \sqrt{3g}$ , evaluates to

$$H = -\ell_0^{-1} e^{(3t+\lambda)/4} \frac{3 + \lambda_{,t}}{12}. \quad (3.17)$$

As, by Eq. (2.3a),  $\lambda_{,t} \geq 0$ , we thus have  $H < 0$  (i.e., the spacetime is contracting in the direction  $t \rightarrow +\infty$ ). We then find

$$(\mathcal{N}^{-1}, E_1^1) = -12 \left( \frac{1}{3 + \lambda_{,t}}, e^{-t} \frac{1}{3 + \lambda_{,t}} \right), \quad (3.18a)$$

$$(\Sigma_+, \dot{U}) = \left( \frac{3 - \lambda_{,t}}{3 + \lambda_{,t}}, 3 e^{-t} \frac{\lambda_{,x}}{3 + \lambda_{,t}} \right), \quad (3.18b)$$

$$(\Sigma_-, N_\times) = 2\sqrt{3} \left( -\frac{P_{,t}}{3 + \lambda_{,t}}, e^{-t} \frac{P_{,x}}{3 + \lambda_{,t}} \right), \quad (3.18c)$$

$$(\Sigma_\times, N_-) = -2\sqrt{3} \left( e^P \frac{Q_{,t}}{3 + \lambda_{,t}}, e^{-(t-P)} \frac{Q_{,x}}{3 + \lambda_{,t}} \right), \quad (3.18d)$$

and  $R = -\sqrt{3}\Sigma_\times$ . Note that Eq. (3.18a) leads to  $\mathcal{N}E_1^1 = e^{-t}$ , implying that for the metric (2.1) the timelike area and the null cone gauge conditions are simultaneously satisfied (see Ref. [20, §3] for terminology). The latter corresponds to choosing  $t$  to be a wavelike time coordinate.

The auxiliary variables  $q$  and  $r$ , defined in Eqs. (3.3) and (3.4), are given by

$$q = 2 + \frac{12\lambda_{,tt}}{(3 + \lambda_{,t})^2}, \quad r = e^{-t} \frac{3}{3 + \lambda_{,t}} \left( \lambda_{,x} + \frac{4\lambda_{,tx}}{3 + \lambda_{,t}} \right). \quad (3.19)$$

Note that the gauge constraint (3.12a) reduces to an identity when  $r$ ,  $\dot{U}$ ,  $E_1^1$  and  $\Sigma_+$  are substituted by their expressions in terms of  $\lambda$ ,  $P$  and  $Q$ , given in Eqs. (3.19) and (3.18). Thus, this gauge constraint is redundant when formulating the dynamics of Gowdy vacuum spacetimes in terms of the metric variables of Eq. (2.1); it has been solved already.

**3.2. Area expansion rate normalization.** Noting that the variable combination  $(r - \dot{U})$ , as well as the deceleration parameter  $q$ , show up frequently on the right hand sides of the Hubble-normalized evolution equations (3.13), and so making explicit use of the gauge constraint (3.12a) and Eq. (3.15), one finds that (for  $\Sigma_+ \neq -1$ ) it is convenient to introduce variables  $\tilde{E}_1^1$ ,  $\tilde{\Sigma}_-$ ,  $\tilde{\Sigma}_\times$ ,  $\tilde{N}_-$  and  $\tilde{N}_\times$  by

$$(\tilde{E}_1^1, \tilde{\Sigma}_-, \tilde{\Sigma}_\times, \tilde{N}_-, \tilde{N}_\times) := (E_1^1, \Sigma_-, \Sigma_\times, N_-, N_\times)/(1 + \Sigma_+). \quad (3.20)$$

In terms of these variables, Eqs. (3.13) convert into the unconstrained autonomous symmetric hyperbolic evolution system

$$C^{-1}\partial_t \tilde{E}_1^1 = 2\tilde{E}_1^1, \quad (3.21a)$$

$$C^{-1}\partial_t \tilde{\Sigma}_- + \tilde{E}_1^1 \partial_x \tilde{N}_\times = 2\sqrt{3}\tilde{\Sigma}_-^2 - 2\sqrt{3}\tilde{N}_-^2, \quad (3.21b)$$

$$C^{-1}\partial_t \tilde{N}_\times + \tilde{E}_1^1 \partial_x \tilde{\Sigma}_- = 2\tilde{N}_\times, \quad (3.21c)$$

$$C^{-1}\partial_t \tilde{\Sigma}_\times - \tilde{E}_1^1 \partial_x \tilde{N}_- = -2\sqrt{3}\tilde{\Sigma}_- \tilde{\Sigma}_\times - 2\sqrt{3}\tilde{N}_\times \tilde{N}_-, \quad (3.21d)$$

$$C^{-1}\partial_t \tilde{N}_- - \tilde{E}_1^1 \partial_x \tilde{\Sigma}_\times = 2\tilde{N}_- + 2\sqrt{3}\tilde{\Sigma}_- \tilde{N}_- + 2\sqrt{3}\tilde{N}_\times \tilde{\Sigma}_\times, \quad (3.21e)$$

with an auxiliary equation given by

$$C^{-1}\partial_t \left[ \frac{1}{(1 + \Sigma_+)} \right] - \frac{1}{3} \tilde{E}_1^1 \partial_x \left[ \frac{\dot{U}}{(1 + \Sigma_+)} \right] = 2\tilde{N}_\times^2 + 2\tilde{N}_-^2. \quad (3.22)$$

The latter is redundant though, since the variables  $\tilde{U} := \dot{U}/(1 + \Sigma_+)$  and  $\tilde{\Sigma}_+ := \Sigma_+/(1 + \Sigma_+)$  are given algebraically by

$$\tilde{U} = \tilde{r} , \quad (3.23a)$$

$$\tilde{\Sigma}_+ = \frac{1}{2} (1 - \tilde{\Sigma}_-^2 - \tilde{N}_\times^2 - \tilde{\Sigma}_\times^2 - \tilde{N}_-^2) , \quad (3.23b)$$

$$\tilde{r} = -3(\tilde{N}_\times \tilde{\Sigma}_- - \tilde{N}_- \tilde{\Sigma}_\times) , \quad (3.23c)$$

the relations to which Eqs. (3.12) transform. But Eqs. (3.21)–(3.23) are nothing but the Gowdy equations written in terms of the area expansion rate normalized variables of Ref. [20]; it is obtained by appropriately specializing Eqs. (113)–(117) in that paper. The evolution system is well defined everywhere except (i) at  $\Sigma_+ = -1$ , and (ii) (for  $C > 0$ ) in the limit  $t \rightarrow +\infty$ .

We now give the area expansion rate normalized frame and connection variables in terms of the metric variables  $\lambda$ ,  $P$  and  $Q$ , and  $C = -\frac{1}{2}$ . Thus

$$(\tilde{\mathcal{N}}^{-1}, \tilde{E}_1^1) = -2(1, e^{-t}) , \quad (3.24a)$$

$$(\tilde{\Sigma}_+, \tilde{U}) = \frac{1}{2} \left( 1 - \frac{1}{3} \lambda_{,t}, e^{-t} \lambda_{,x} \right) , \quad (3.24b)$$

$$(\tilde{\Sigma}_-, \tilde{N}_\times) = \frac{1}{\sqrt{3}} (-P_{,t}, e^{-t} P_{,x}) , \quad (3.24c)$$

$$(\tilde{\Sigma}_\times, \tilde{N}_-) = -\frac{1}{\sqrt{3}} (e^P Q_{,t}, e^{-(t-P)} Q_{,x}) , \quad (3.24d)$$

and  $\tilde{R} = -\sqrt{3}\tilde{\Sigma}_\times$  (see also Ref. [20, §A.3]).

We will employ the Hubble-normalized variables and equations in the discussion which follows.

#### 4. INVARIANT SETS

For the Hubble-normalized orthonormal frame representation of the system of equations describing the dynamics of Gowdy vacuum spacetimes, given by Eqs. (3.12)–(3.14), it is straightforward to identify several invariant sets. The most notable ones are:

- (1) Gowdy vacuum spacetimes with

$$0 = \Sigma_\times = N_- ,$$

referred to as the *polarized invariant set*,

- (2) Vacuum spacetimes that are spatially self-similar (SSS) in the sense of Eardley [15, §3], given by

$$\mathbf{0} = \partial_x \mathbf{X} , \quad \dot{U} = r ,$$

and  $\dot{U}$  and  $r$  as in Eqs. (3.12c) and (3.4). We refer to these as the *SSS invariant set*. Within the SSS invariant set we find as another subset spatially homogeneous (SH) vacuum spacetimes, obtained by setting  $0 = \dot{U} = r$ . These form the *SH invariant set*.

(3) the invariant set given by

$$0 = E_1^1 ,$$

which, following Ref. [38, §3.2.3], we refer to as the *silent boundary*.

Note that for the *plane symmetric invariant set*, defined by  $0 = \Sigma_\times = N_- = \Sigma_- = N_\times$ , one has  $\Sigma_+ = \pm 1$  due to the Gauß constraint (3.12b);  $\Sigma_+ = -1$  yields a locally Minkowski solution, while  $\Sigma_+ = 1$  yields a non-flat plane symmetric locally Kasner solution. Thus, contrary to some statements in the literature, general Gowdy vacuum spacetimes are not plane symmetric.

There exists a deep connection between the SSS invariant set and the silent boundary: in the SSS case the evolution equation (3.13a) for  $E_1^1$  decouples and leaves a reduced system of equations for the remaining variables<sup>9</sup>; the evolution equations in this reduced system are identical to those governing the dynamics on the silent boundary, obtained by setting  $E_1^1 = 0$ . The reduced system thus describes the essential dynamical features of the SSS problem. In contrast to the true SSS and SH cases, the variables on the silent boundary are  $x$ -dependent; thus orbits on the silent boundary do not in general correspond to exact solutions of Einstein's field equations. As will be shown, the silent boundary plays a key rôle in the asymptotic analysis towards the singularity of the Hubble-normalized system of equations. Therefore, we now take a more detailed look at the silent boundary and some of its associated invariant subsets.

**4.1. Silent boundary.** Setting  $E_1^1 = 0$  in the Hubble-normalized system of equations (3.12)–(3.14) describing Gowdy vacuum spacetimes (and hence cancelling all terms involving  $E_1^1 \partial_x$ ), reduces it to the system of constraints

$$(r - \dot{U}) = 0 , \quad (4.1a)$$

$$1 = \Sigma_+^2 + \Sigma_-^2 + \Sigma_\times^2 + N_\times^2 + N_-^2 , \quad (4.1b)$$

$$(1 + \Sigma_+) \dot{U} = -3(N_\times \Sigma_- - N_- \Sigma_\times) , \quad (4.1c)$$

and evolution equations

$$C^{-1}(1 + \Sigma_+) \partial_t(1 + \Sigma_+) = (q - 2)(1 + \Sigma_+) , \quad (4.2a)$$

$$C^{-1}(1 + \Sigma_+) \partial_t \Sigma_- = (q - 2)\Sigma_- + 2\sqrt{3}\Sigma_\times^2 - 2\sqrt{3}N_-^2 , \quad (4.2b)$$

$$C^{-1}(1 + \Sigma_+) \partial_t N_\times = (q + 2\Sigma_+) N_\times , \quad (4.2c)$$

$$C^{-1}(1 + \Sigma_+) \partial_t \Sigma_\times = (q - 2 - 2\sqrt{3}\Sigma_-)\Sigma_\times - 2\sqrt{3}N_\times N_- , \quad (4.2d)$$

$$C^{-1}(1 + \Sigma_+) \partial_t N_- = (q + 2\Sigma_+ + 2\sqrt{3}\Sigma_-)N_- + 2\sqrt{3}N_\times \Sigma_\times , \quad (4.2e)$$

with

$$q = 2(\Sigma_+^2 + \Sigma_-^2 + \Sigma_\times^2) . \quad (4.3)$$

The integrability condition (3.5) reduces to

$$C^{-1}(1 + \Sigma_+) \partial_t r = (q + 2\Sigma_+) r . \quad (4.4)$$

---

<sup>9</sup>The variable  $E_1^1$  only appears as part of the spatial frame derivative  $E_1^1 \partial_x$  in the equations for these variables; the SSS requirement implies that these terms have to be dropped. We discuss these issues again in Sec. 6.

In the above system, the variables  $\dot{U}$  and  $r$  decouple, and so Eqs. (4.1a), (4.1c) and (4.4) can be treated separately; the remaining autonomous system thus contains the key dynamical information. Note that it follows from Eqs. (4.2c) and (4.4) that  $r$  is proportional to  $N_\times$ , with an  $x$ -dependent proportionality factor. This is not a coincidence: for the corresponding SSS equations the square of this factor is proportional to the *constant* self-similarity parameter  $f$ , defined in Ref. [15, p. 294].

On the silent boundary we see a great simplification: firstly, the system is reduced from a system of partial differential equations to one of ordinary differential equations; secondly, the reduction of the gauge constraint (3.12a) to Eq. (4.1a) yields a decoupling of  $\dot{U}$  and  $r$ ; note, however, that the Gauß and Codacci constraints, Eqs. (3.12b) and (3.12c), remain *unchanged*.

We will see in Sec. 5 below that the “silent equations,” Eqs. (3.12b), (3.12c), (4.2) and (4.3), significantly influence and govern the asymptotic dynamics of Gowdy vacuum spacetimes in the approach to the singularity.

4.1.1. *Polarized set on the silent boundary.* Taking the intersection between the polarized invariant set ( $0 = \Sigma_\times = N_\times$ ) and the silent boundary ( $0 = E_1^1$ ) yields:

$$1 = \Sigma_+^2 + \Sigma_-^2 + N_\times^2, \quad (4.5a)$$

$$(1 + \Sigma_+) \dot{U} = -3\Sigma_- N_\times = (1 + \Sigma_+) r, \quad (4.5b)$$

and

$$C^{-1} \partial_t (1 + \Sigma_+) = -2N_\times^2, \quad (4.6a)$$

$$C^{-1} (1 + \Sigma_+) \partial_t N_\times = 2 \left[ \left( \Sigma_+ + \frac{1}{2} \right)^2 + \Sigma_-^2 - \frac{1}{4} \right] N_\times, \quad (4.6b)$$

$$\Sigma_- = \text{constant} \times (1 + \Sigma_+). \quad (4.6c)$$

Note that with  $C < 0$ ,  $N_\times$  increases to the future when  $(\Sigma_+, \Sigma_-)$  take values inside a disc of radius  $\frac{1}{2}$  centered on  $(-\frac{1}{2}, 0)$  in the  $(\Sigma_+ \Sigma_-)$ -plane of the Hubble-normalized state space, and decreases outside of it. Note also that the projections into the  $(\Sigma_+ \Sigma_-)$ -plane of the orbits determined by these equations constitute a 1-parameter family of straight lines that emanate from the point  $(-1, 0)$  (which we will later refer to as the Taub point  $T_1$ ).

4.2. **SH invariant set.** By setting  $0 = \dot{U} = r$  one obtains the SH invariant set as a subset of the SSS invariant set. Since in the present case  $n_{\alpha\beta} n^{\alpha\beta} - (n_\alpha^\alpha)^2 \geq 0$ , it follows that this invariant set contains vacuum Bianchi models of Type-I, Type-II and Type-VI<sub>0</sub> only (see King and Ellis [30, p. 216]), though in general not in the canonical frame representation of Ellis and MacCallum [17] (presently the spatial frame  $\{e_\alpha\}$  is *not* an eigenframe of  $N_{\alpha\beta}$ , *nor* is it Fermi propagated along  $e_0$ ). However, the conversion to the latter can be achieved by a time dependent global rotation of the spatial frame about  $e_1$ . Note that the present representation means that there exists only one reduction (Lie contraction) from Type-VI<sub>0</sub> to Type-II, in contrast to the diagonal representation where there exist two possible reductions. This has the consequence that the dynamics

of Gowdy vacuum spacetimes allows only for the existence of a single kind of curvature transition (see Sec. 5), described by the Taub invariant set introduced below.

The SH restrictions,  $\mathbf{0} = \partial_x \mathbf{X}$  and  $0 = \dot{U} = r$ , yield the constraints

$$1 = \Sigma_+^2 + \Sigma_-^2 + \Sigma_\times^2 + N_\times^2 + N_-^2 , \quad (4.7a)$$

$$0 = N_\times \Sigma_- - N_- \Sigma_\times , \quad (4.7b)$$

and the evolution equations (4.2), with Eq. (4.3), and the decoupled evolution equation for  $E_1^1$ , Eq. (3.13a).

4.2.1. *Taub invariant set.* The Taub invariant set, a set of SH vacuum solutions of Bianchi Type-II, is defined as the subset

$$0 = \Sigma_\times = N_\times$$

of Eqs. (4.7), (4.2) and (4.3). This leads to the reduced system of equations

$$1 = \Sigma_+^2 + \Sigma_-^2 + N_-^2 , \quad (4.8)$$

and

$$C^{-1}(1 + \Sigma_+) \partial_t(1 + \Sigma_+) = (q - 2)(1 + \Sigma_+) , \quad (4.9a)$$

$$C^{-1}(1 + \Sigma_+) \partial_t \Sigma_- = (q - 2) \Sigma_- - 2\sqrt{3} N_-^2 , \quad (4.9b)$$

$$C^{-1}(1 + \Sigma_+) \partial_t N_- = (q + 2\Sigma_+ + 2\sqrt{3}\Sigma_-) N_- , \quad (4.9c)$$

with

$$q = 2(\Sigma_+^2 + \Sigma_-^2) . \quad (4.10)$$

On account of employing Eq. (4.8) in Eq. (4.10), one finds from Eqs. (4.9a) and (4.9b) that the Taub orbits are represented in the  $(\Sigma_+ \Sigma_-)$ -plane of the Hubble-normalized state space by a 1-parameter family of straight lines, i.e.,

$$\Sigma_- = \text{constant} \times (1 + \Sigma_+) - \sqrt{3} , \quad (4.11)$$

(see WE, Subsec. 6.3.2, for further details).

4.2.2. *Kasner invariant set.* The Kasner invariant set, a set of SH vacuum solutions of Bianchi Type-I, is defined as the subset

$$0 = N_\times = N_-$$

of Eqs. (4.7), (4.2) and (4.3). This leads to the reduced system of equations

$$1 = \Sigma_+^2 + \Sigma_-^2 + \Sigma_\times^2 , \quad (4.12)$$

and

$$C^{-1}(1 + \Sigma_+) \partial_t(1 + \Sigma_+) = 0 , \quad (4.13a)$$

$$C^{-1}(1 + \Sigma_+) \partial_t \Sigma_- = 2\sqrt{3} \Sigma_\times^2 , \quad (4.13b)$$

$$C^{-1}(1 + \Sigma_+) \partial_t \Sigma_\times = -2\sqrt{3} \Sigma_- \Sigma_\times , \quad (4.13c)$$

with

$$q = 2 . \quad (4.14)$$

These equations define a flow on the unit sphere in  $\Sigma$ -space, with coordinates  $(\Sigma_+, \Sigma_-, \Sigma_\times)$ , which we refer to as the *Kasner sphere*. The Kasner orbits on

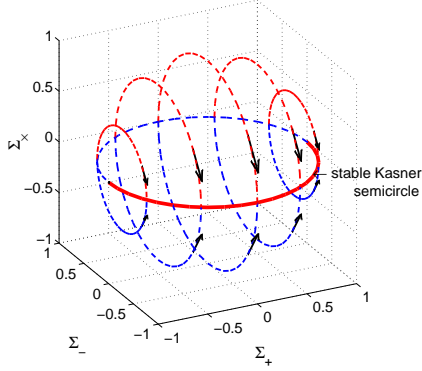


FIG. 1. The flow on the Kasner sphere.

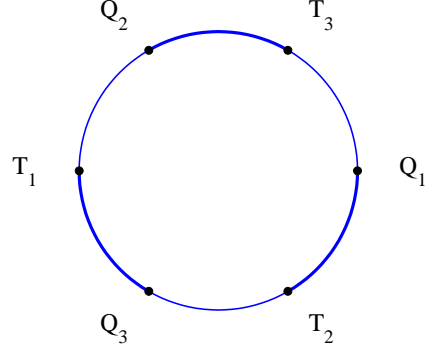


FIG. 2. The special points on the Kasner circle.

this sphere represent Kasner solutions with respect to a spatial frame that is *not* Fermi propagated along  $e_0$ ; such orbits are depicted in Fig. 1. The projections of the Kasner orbits into the  $(\Sigma_+\Sigma_-)$ -plane of the Hubble-normalized state space form a 1-parameter family of parallel straight lines, given by

$$\Sigma_+ = \text{constant} . \quad (4.15)$$

The subset of Kasner orbits that represent Kasner solutions with respect to a spatial frame that *is* Fermi propagated along  $e_0$  is given by [cf. Eq. (3.11)]

$$0 = \Sigma_x , \quad (4.16)$$

thus giving rise to a *unit circle of equilibrium points* in the  $(\Sigma_+\Sigma_-)$ -plane described by

$$1 = \Sigma_+^2 + \Sigma_-^2 , \quad 0 = \partial_t \Sigma_+ = \partial_t \Sigma_- . \quad (4.17)$$

This set of equilibrium points forms the familiar *Kasner circle*, denoted by

$$\mathcal{K} .$$

The Kasner exponents in the equilibrium state are given by (WE, Subsec. 6.2.2)

$$p_1 = \frac{1}{3} (1 - 2\Sigma_+) , \quad p_{2,3} = \frac{1}{3} \left( 1 + \Sigma_+ \pm \sqrt{3}\Sigma_- \right) . \quad (4.18)$$

Note that according to an ordering given by  $p_1 < p_2 < p_3$  and its permutations,  $\mathcal{K}$  subdivides into six equivalent sectors. The sectors are separated by special



points for which the variable pair  $(\Sigma_+, \Sigma_-)$  takes the fixed values

$$\begin{aligned} Q_1 &: (1, 0) , & T_3 &: \left( \frac{1}{2}, \frac{\sqrt{3}}{2} \right) , \\ Q_2 &: \left( -\frac{1}{2}, \frac{\sqrt{3}}{2} \right) , & T_1 &: (-1, 0) , \\ Q_3 &: \left( -\frac{1}{2}, -\frac{\sqrt{3}}{2} \right) , & T_2 &: \left( \frac{1}{2}, -\frac{\sqrt{3}}{2} \right) , \end{aligned}$$

so that two of the Kasner exponents become equal. The points  $Q_\alpha$  correspond to Kasner solutions that are locally rotationally symmetric, while the points  $T_\alpha$  correspond to Taub's representation of the Minkowski solution (see WE, Subsec. 6.2.2, for further details).

## 5. ASYMPTOTIC DYNAMICS TOWARDS THE SINGULARITY

**5.1. Description using metric variables.** In this subsection we will briefly review the dynamical phenomenology of Gowdy vacuum spacetimes as described by the system of equations (2.2) for the metric variables  $\lambda$ ,  $P$  and  $Q$ ; this was discussed earlier by Berger and Moncrief [8] and Berger and Garfinkle [5] on the basis of extensive numerical experiments. In the following we reproduce some of their results, using LeVeque's CLAWPACK<sup>10</sup>; see Ref. [31] for background. Employing the "standing wave" initial data of Ref. [8],

$$\begin{aligned} P(0, x) &= 0 , & P_{,t}(0, x) &= 5 \cos x , \\ Q(0, x) &= \cos x , & Q_{,t}(0, x) &= 0 , \\ \lambda(0, x) &= 0 , \end{aligned}$$

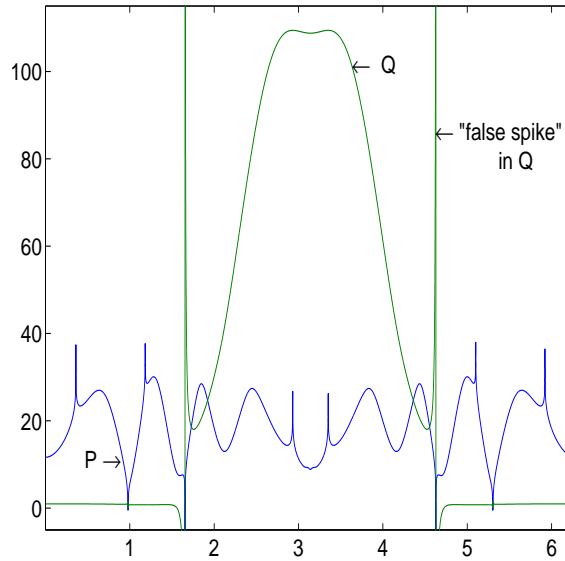
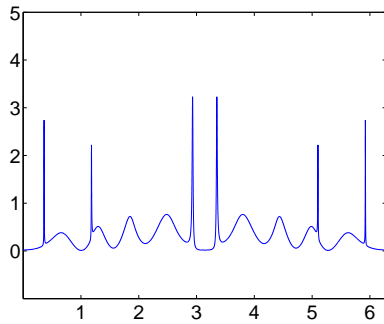
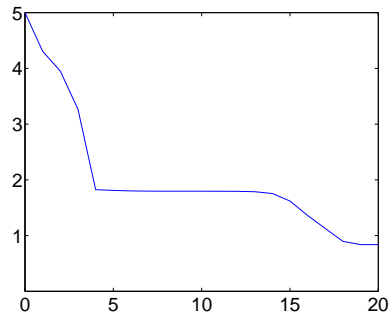
our integration proceeds on a 1-dimensional spatial grid representing the  $x$ -interval  $(0, 2\pi)$ , of step size  $0.2 \times 10^{-3}$  (thus there are 31416 spatial points; end points identified), with a time step size of  $0.2 \times 10^{-3}$ .

In our analysis we are only concerned with the direction towards the singularity, which, with our choice of area time coordinate, corresponds to  $t \rightarrow +\infty$ . In this regime, because of the factors  $e^{-2t}$  accompanying the spatial derivatives in Eqs. (2.2), it is plausible that the evolution along different timelines (each of which being given by  $x = \text{constant}$ ) decouples. As is well known, in the approach to the singularity the metric variables  $P$  and  $Q$  (as functions of  $t$  and  $x$ ) develop so-called "spiky features"; see Fig. 3 for a plot at a fixed  $t$ .

The apparent discontinuities in  $Q$  at certain values of  $x$  develop along exceptional timelines for which  $Q_{,t} = 0$ . They are induced by local minima in  $P$  with  $P < 0$ . The latter are known to be coordinate (gauge) effects and are hence referred to by Rendall and Weaver [34] as "false spikes".

The sharp local maxima in  $P$  with  $P > 0$ , on the other hand, develop along exceptional timelines for which  $Q_{,x} = 0$ . That is,  $Q$  exhibits smooth behavior along such timelines. The upward pointing peaks in  $P$  are known to have a

<sup>10</sup>This package is available from the URL: <http://www.amath.washington.edu/~claw/>.

FIG. 3.  $P$  and  $Q$  at  $t = 40$ .FIG. 4.  $\lambda_{,t}$  at  $t = 10$ .FIG. 5. Time evolution of  $\max_x v$ .

geometrical origin and are hence referred to by Rendall and Weaver [34] as “true spikes”.

In terms of the hyperbolic space geometry, the false spikes correspond to points on a loop in  $\mathbf{H}^2$ , evolving under the Gowdy equations, which travel towards a point on the conformal boundary of  $\mathbf{H}^2$  chosen as infinity in passing to the model given by the metric (2.5). On the other hand, the true spikes correspond to points located on cusps of the loop, which travel at higher velocity than the rest of the loop.

Note that while the coordinate derivative quantities  $\lambda_{,t}$  and  $P_{,t}$  are scale-invariant,  $P_{,x}$ ,  $Q_{,t}$  and  $Q_{,x}$  are not. Examples of geometrically defined quantities are the hyperbolic velocity and the hyperbolic norm of the spatial derivative, which, with  $u(t, x)$  representing the point in  $\mathbf{H}^2$ , are given by

$$v(t, x) = \|\partial_t u\|_{g_{\mathbf{H}^2}} \ , \quad e^{-t} \|\partial_x u\|_{g_{\mathbf{H}^2}} \ .$$

Since we are using a logarithmic time coordinate, these two quantities are scale-invariant by construction. One is inexorably led to consider the scale-invariant operators  $\partial_t$  and  $e^{-t} \partial_x$ . In terms of the dimensional time coordinate  $\tau = \ell_0 e^{-t}$ , these operators are  $-\tau \partial_\tau$  and  $\tau \partial_x$ , respectively.

The “energy density”,  $\lambda_{,t}$ , depicted at a fixed  $t$  in Fig. 4, decreases more slowly at spike points. Since we are not using an adaptive solver, we are not able to numerically resolve the behavior of  $\lambda_{,t}$  at spike points. With  $u(t, x)$  representing the point in  $\mathbf{H}^2$ , however, we have from the Gauß constraint (2.3a)

$$\lambda_{,t}(t, x) = v^2(t, x) + e^{-2t} \|\partial_x u\|_{g_{\mathbf{H}^2}}^2 ,$$

where the second term is expected to tend to zero pointwise. Therefore, we expect that  $\lambda_{,t}$  asymptotically tends to a nonzero limit pointwise, given by the asymptotic hyperbolic velocity which we define as

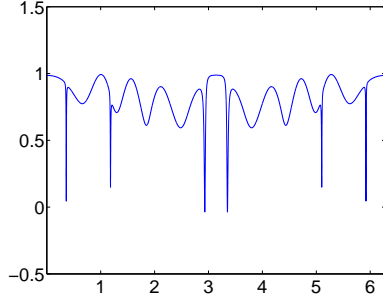
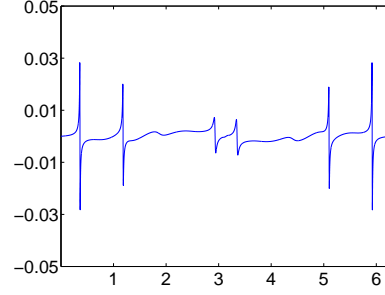
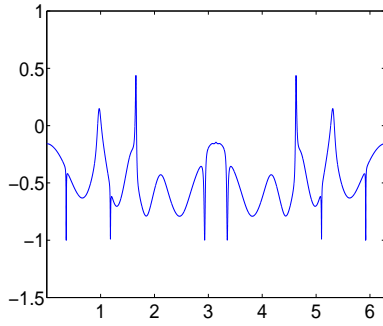
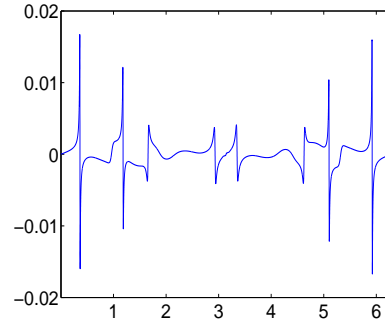
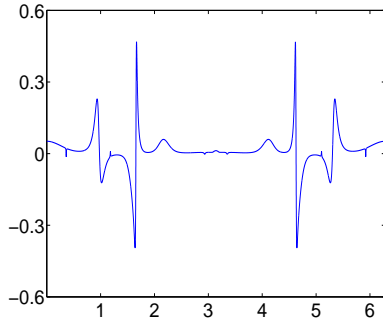
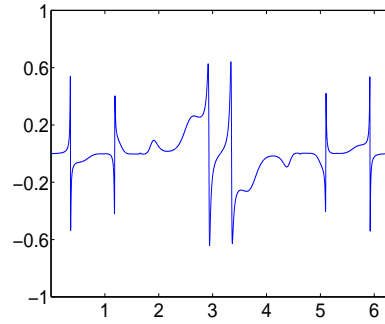
$$\hat{v}(x) := \lim_{t \rightarrow +\infty} v(t, x) , \quad (5.1)$$

where the limit exists. As argued by Berger and Moncrief [8] and Berger and Garfinkle [5], the dynamics force the hyperbolic velocity to values  $v \leq 1$  at late times, except along timelines where spikes form; see Fig. 5. The reason  $\max_x v$  appears to be less than 1 at late times in Fig. 5 is that the spikes have become so narrow that they are not resolved numerically.

Rendall and Weaver [34] have shown how to construct Gowdy solutions with both false and true spikes from smooth solutions by a hyperbolic inversion followed by an Ernst transformation. In particular, they show that along those exceptional timelines,  $x = x_{t\text{Spike}}$ , where (in numerical simulations) true spikes form as  $t \rightarrow +\infty$ , the asymptotic hyperbolic velocity satisfies  $\hat{v}(x_{t\text{Spike}}) = 1 + s$ , with  $s \in (0, 1)$ . On the other hand, along nearby, typical, timelines the limiting value is  $\hat{v} = 1 - s$ . The speed at which  $v$  approaches  $\hat{v} = 1 - s$  along the latter timelines decreases rapidly as  $x$  approaches  $x_{t\text{Spike}}$ . For the exceptional timelines,  $x = x_{f\text{Spike}}$ , where (in numerical simulations) false spikes form as  $t \rightarrow +\infty$ , the asymptotic hyperbolic velocity satisfies  $\hat{v}(x_{f\text{Spike}}) = s$ , again with  $s \in (0, 1)$ . Nearby, typical, timelines have limiting velocities  $\hat{v}$  close to  $s$ . The regimes  $1 < \hat{v}(x_{t\text{Spike}}) < 2$  and  $0 < \hat{v}(x_{f\text{Spike}}) < 1$  are referred to by Garfinkle and Weaver [21] as the regimes of “low velocity spikes”.

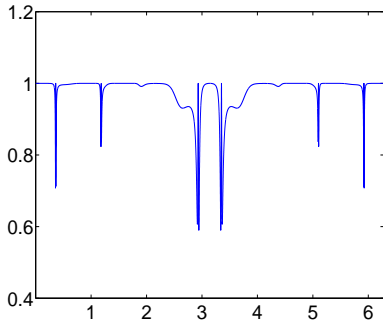
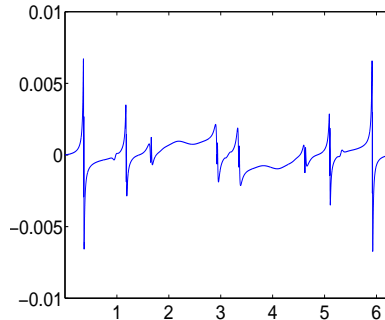
The true spikes with  $\hat{v}(x_{t\text{Spike}}) \in (1, 2)$  correspond, as has been known for a long time, to simple zeros of  $Q_{,x}$ . Higher velocity spikes were also constructed by Rendall and Weaver. However, these correspond to higher order zeros of  $Q_{,x}$ , and are therefore nongeneric.

**5.2. Description using Hubble-normalized variables.** Here we first describe the behavior of the Hubble-normalized variables  $\Sigma_+$ ,  $\Sigma_-$ ,  $N_x$ ,  $\Sigma_x$ ,  $N_-$  and  $\dot{U}$ , when expressed in terms of the metric variables  $\lambda$ ,  $P$  and  $Q$  and their coordinate derivatives as in Eqs. (3.18), under the numerical integration of the Gowdy equations (2.2)–(2.3). We use the same “standing wave” initial data as in Subsec. 5.1. The spatial variation of the values of the Hubble-normalized variables at a fixed  $t$  is depicted in Figs. 6–11. Note, in particular, the scales along the vertical axes in these figures.

FIG. 6.  $\Sigma_+$  at  $t = 10$ .FIG. 7.  $\dot{U}$  at  $t = 10$ .FIG. 8.  $\Sigma_-$  at  $t = 10$ .FIG. 9.  $N_\times$  at  $t = 10$ .FIG. 10.  $\Sigma_\times$  at  $t = 10$ .FIG. 11.  $N_-$  at  $t = 10$ .

As we see in Figs. 7 and 9,  $\dot{U}$  and  $N_\times$  become uniformly small as  $t$  increases. On the other hand,  $\Sigma^2$  tends to the value 1 almost everywhere except along those timelines where either a false or a true spike is being formed; see Fig. 12. Further, while  $\Sigma_\times$  and  $N_-$  do not necessarily become small individually as  $t$  increases, see Figs. 10 and 11, their mutual product  $N_- \Sigma_\times$ , nevertheless, does; see Fig. 13. Relating these observations and the analytic result (derivable from Subsec. 3.1) that

$$|E_1^1| \leq 4e^{-t}, \quad (5.2)$$


 FIG. 12.  $\Sigma^2$  at  $t = 10$ .

 FIG. 13.  $N_{\Sigma_x}$  at  $t = 10$ .

so  $E_1^1 \rightarrow 0$  uniformly as  $t \rightarrow +\infty$ , to the system of equations (3.12)–(3.14) suggests that, in the approach to the singularity, for Gowdy vacuum spacetimes the ultra-strong spacetime curvature phenomenon of *asymptotic silence*, described in Refs. [20, §5.3] and [38, §4.1], sets in. Asymptotic silence refers to the collapse of the local null cones onto the timelines as  $t \rightarrow +\infty$ , with the physical consequence that the propagation of gravitational waves between neighboring timelines is gradually frozen in. Based on these considerations, it is natural to expect that near the singularity the spatial derivatives of the Hubble-normalized connection variables become dynamically irrelevant, and that thus, in a neighborhood of the silent boundary of the Hubble-normalized state space, the dynamics of Gowdy vacuum spacetimes is well approximated by the dynamics on the silent boundary. More precisely, it is well approximated by the system of equations (3.12b), (3.12c), (4.2), (4.3) and (4.1a), but note that the Hubble-normalized variables are now  $x$ -dependent. This aspect of the asymptotic dynamics may also be viewed as a consequence of the friction term  $\tau^{-1} \partial_\tau$  in Eq. (2.6). In Figs. 14 and 15 we show the projections into the  $(\Sigma_+ \Sigma_-)$ -plane of the Hubble-normalized state space of orbits for (i) the evolution system on the silent boundary, Eqs. (4.2), and (ii) a typical timeline of the full Gowdy evolution equations (3.13). It is apparent that *qualitative features of the full Gowdy evolution system along an individual timeline are correctly reproduced by the evolution system on the silent boundary*.

To gain further insight into the dynamics towards the singularity, we will now investigate the local stability of the Kasner circle  $\mathcal{K}$  on the silent boundary of the Hubble-normalized state space for Gowdy vacuum spacetimes, thus probing the closest parts of the interior of the state space.

5.2.1. *Linearized dynamics at the Kasner circle on the silent boundary.* We recall that on the silent boundary the Hubble-normalized variables are  $x$ -dependent. Consequently, the Kasner circle  $\mathcal{K}$  on the silent boundary is represented by the conditions

$$0 = E_1^1 = \Sigma_x = N_x = N_- = \dot{U} = r, \quad \Sigma_+ = \hat{\Sigma}_+, \quad \Sigma_- = \hat{\Sigma}_-, \quad (5.3a)$$

$$1 = \hat{\Sigma}_+^2 + \hat{\Sigma}_-^2, \quad q = 2, \quad (5.3b)$$

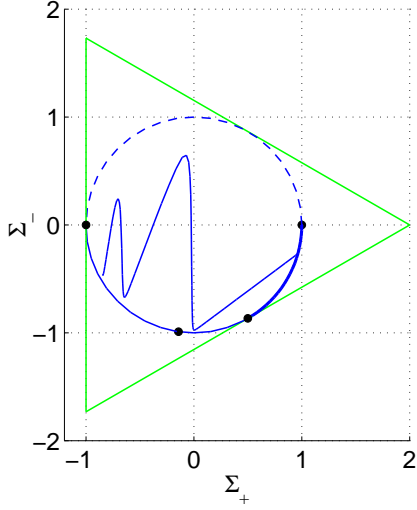


FIG. 14. Projection into the  $(\Sigma_+\Sigma_-)$ -plane of an orbit determined by the SB system (4.2).

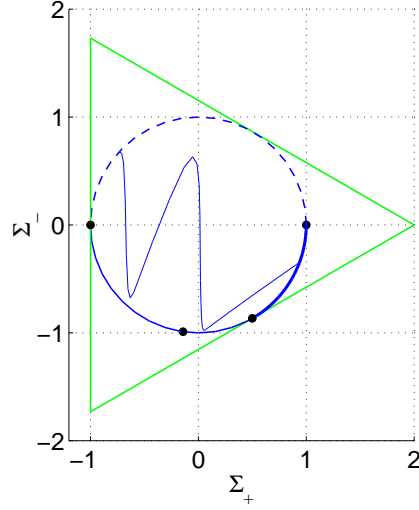


FIG. 15. Projection into the  $(\Sigma_+\Sigma_-)$ -plane of a Gowdy orbit along the typical timeline  $x = 2.7$ .

where we introduce the convention that “hatted” variables are functions of the spatial coordinate  $x$  only. Thus, linearizing the Hubble-normalized Gowdy evolution equations (3.13) on the silent boundary at an equilibrium point  $(\hat{\Sigma}_+, \hat{\Sigma}_-)$  of  $\mathcal{K}$  yields (with  $C = -\frac{1}{2}$ )

$$\partial_t E_1^1 = -E_1^1, \quad (5.4a)$$

$$\partial_t \delta\Sigma_+ = -2(\hat{\Sigma}_+ \delta\Sigma_+ + \hat{\Sigma}_- \delta\Sigma_-), \quad (5.4b)$$

$$\partial_t \delta\Sigma_- = -2 \frac{\hat{\Sigma}_-}{(1 + \hat{\Sigma}_+)} (\hat{\Sigma}_+ \delta\Sigma_+ + \hat{\Sigma}_- \delta\Sigma_-), \quad (5.4c)$$

$$\partial_t N_\times = -N_\times + \frac{1}{2} \frac{\partial_x \hat{\Sigma}_-}{(1 + \hat{\Sigma}_+)} E_1^1, \quad (5.4d)$$

$$\partial_t \Sigma_\times = \frac{\sqrt{3}\hat{\Sigma}_-}{(1 + \hat{\Sigma}_+)} \Sigma_\times, \quad (5.4e)$$

$$\partial_t N_- = - \left[ 1 + \frac{\sqrt{3}\hat{\Sigma}_-}{(1 + \hat{\Sigma}_+)} \right] N_-; \quad (5.4f)$$

here  $\delta\Sigma_+$  and  $\delta\Sigma_-$  denote the deviations in  $\Sigma_+$  and  $\Sigma_-$  from their equilibrium values  $\hat{\Sigma}_+$  and  $\hat{\Sigma}_-$  on  $\mathcal{K}$ . Let us define an  $x$ -dependent function

$$k(x) := - \frac{\sqrt{3}\hat{\Sigma}_-(x)}{1 + \hat{\Sigma}_+(x)}, \quad (5.5)$$

corresponding to a particular function used in Refs. [29] and [34]. Then, integrating Eqs. (5.4) with respect to  $t$ , we find for  $E_1^1$ ,  $\delta\Sigma_+$ ,  $\delta\Sigma_-$  and  $N_\times$

$$E_1^1 = \mathcal{O}(e^{-t}) , \quad (5.6a)$$

$$\delta\Sigma_+ = \mathcal{O}(e^{-t}) , \quad (5.6b)$$

$$\delta\Sigma_- = \mathcal{O}(e^{-t}) , \quad (5.6c)$$

$$N_\times = \hat{N}_\times e^{-t} + \mathcal{O}(te^{-t}) . \quad (5.6d)$$

That is, as  $t \rightarrow +\infty$ , the solutions for  $E_1^1$ ,  $\delta\Sigma_+$  and  $\delta\Sigma_-$  decay exponentially fast as  $e^{-t}$ , while  $N_\times$  decays exponentially fast as  $te^{-t}$ , independent of the values of  $(\hat{\Sigma}_+, \hat{\Sigma}_-)$  [and so  $k(x)$ ] along an individual timeline. Consequently, these variables are stable on  $\mathcal{K}$ . The solutions for the variable pair  $(\Sigma_\times, N_-)$  associated with the “ $\times$ -polarization state”, on the other hand, are given by

$$\Sigma_\times = \hat{\Sigma}_\times e^{-k(x)t} , \quad (5.7a)$$

$$N_- = \hat{N}_- e^{-[1-k(x)]t} , \quad (5.7b)$$

(see also Eqs. (140) and (141) in Ref. [20]).<sup>11</sup> Thus,

- (1)  $\Sigma_\times$  is an unstable variable on  $\mathcal{K}$  as  $t \rightarrow +\infty$  whenever  $k(x) < 0$ ; this happens along timelines for which the values of  $(\hat{\Sigma}_+, \hat{\Sigma}_-)$  define a point on the upper semicircle of  $\mathcal{K}$  (unless, of course,  $0 = \hat{\Sigma}_\times$  along such a timeline), and
- (2)  $N_-$  is an unstable variable on  $\mathcal{K}$  as  $t \rightarrow +\infty$  whenever  $k(x) > 1$ ; this happens along timelines for which the values of  $(\hat{\Sigma}_+, \hat{\Sigma}_-)$  define a point either on the  $\text{arc}(T_1Q_3) \subset \mathcal{K}$  or on the  $\text{arc}(Q_3T_2) \subset \mathcal{K}$  (unless, of course,  $0 = \hat{N}_-$  along such a timeline).

This implies that in the approach to the singularity, the Kasner equilibrium set  $\mathcal{K}$  in the Hubble-normalized state space of every individual timeline has a *1-dimensional unstable manifold*, except when the values of  $(\hat{\Sigma}_+, \hat{\Sigma}_-)$  coincide with those of the special points  $Q_\alpha$  and  $T_\alpha$ , or correspond to points on the  $\text{arc}(T_2Q_1) \subset \mathcal{K}$  which is stable.<sup>12</sup>

Close to the singularity (and so to the silent boundary of the state space), it follows that along those timelines where  $(\hat{\Sigma}_+, \hat{\Sigma}_-)$  take values in the  $\Sigma_\times$ -unstable sectors of  $\mathcal{K}$ , a *frame transition orbit* of Bianchi Type-I according to Eq. (4.15) to the  $\Sigma_\times$ -stable part of  $\mathcal{K}$  is induced (corresponding to a rotation of the spatial frame by  $\pi/2$  about the  $\mathbf{e}_1$ -axis). Notice that timelines along which  $0 = \hat{\Sigma}_\times$  do not participate in these frame transitions and so are “left behind” by the asymptotic dynamics. This provides a simple mechanism for the gradual formation of false spikes on  $\mathbf{T}^3$ . As, by Eq. (3.11),  $\Sigma_\times$  quantifies the Hubble-normalized angular velocity at which  $\mathbf{e}_2$  and  $\mathbf{e}_3$  rotate about  $\mathbf{e}_1$  (the latter being a spatial frame gauge variable), false spikes clearly are a gauge effect.

<sup>11</sup>Altogether, the linear solutions contain four arbitrary  $2\pi$ -periodic real-valued functions of  $x$ , namely  $k$ ,  $\hat{N}_\times$ ,  $\hat{\Sigma}_\times$  and  $\hat{N}_-$ .

<sup>12</sup>For the polarized invariant set, on the other hand, here included as the special case  $0 = \hat{\Sigma}_\times = \hat{N}_-$ , the entire Kasner equilibrium set  $\mathcal{K}$  is stable.

On the other hand, along those timelines where  $(\hat{\Sigma}_+, \hat{\Sigma}_-)$  take values in the  $N_-$ -unstable sectors of  $\mathcal{K}$ , a *curvature transition orbit* of Bianchi Type-II according to Eq. (4.11) to the  $N_-$ -stable part of  $\mathcal{K}$  is induced; this is shown in Fig. 16. Notice that timelines along which  $0 = \hat{N}_-$  do not participate in these curvature transitions and so are “left behind” by the asymptotic dynamics. This provides a simple mechanism for the gradual formation of true spikes on  $\mathbf{T}^3$ . As  $N_-$  presently relates to the intrinsic curvature of  $\mathbf{T}^3$ , true spikes are a geometrical effect.

It was pointed out in Ref. [38, §4.1] that it is natural to expect from the consideration of asymptotic silence that

$$\lim_{t \rightarrow +\infty} E_1^{-1} \partial_x \mathbf{Y} = \mathbf{0} \quad (5.8)$$

is satisfied along typical timelines; in our case  $\mathbf{Y} = (\Sigma_+, \Sigma_-, N_\times, \Sigma_\times, N_-)^T$ . This limit is certainly attained for each of  $\Sigma_+$ ,  $\Sigma_-$  and  $N_\times$  when we use the linear solutions of Eqs. (5.6) for these variables which are valid in a neighborhood of  $\mathcal{K}$  on the silent boundary. For the “ $\times$ -polarization variables”  $(\Sigma_\times, N_-)$  an analogous substitution from Eqs. (5.7) leads to

$$E_1^{-1} \partial_x \Sigma_\times \propto \left( \partial_x \hat{\Sigma}_\times - t \hat{\Sigma}_\times \partial_x k(x) \right) e^{-[1+k(x)]t}, \quad (5.9a)$$

$$E_1^{-1} \partial_x N_- \propto \left( \partial_x \hat{N}_- + t \hat{N}_- \partial_x k(x) \right) e^{-[2-k(x)]t}. \quad (5.9b)$$

Here a number of cases arise when we consider the behavior of these spatial derivative expressions in the limit  $t \rightarrow +\infty$ . Firstly, both decay exponentially fast along those timelines for which the dynamics has entered the regime  $0 \leq k(x) < 1$ . As discussed in some detail below, this happens asymptotically along typical timelines. Secondly, along timelines where false spikes ( $0 = \hat{\Sigma}_\times$ ) form, both decay exponentially fast when the dynamics is confined to the regime  $-1 < k(x) < 0$ . Thirdly, along timelines where true spikes ( $0 = \hat{N}_-$ ) form, both decay exponentially fast when the dynamics is confined to the regime  $1 < k(x) < 2$ . Outside the regime  $-1 < k(x) < 2$ , one or the other of the spatial derivative expressions (5.9) may grow temporarily along timelines, until one of the unstable modes (5.7) drives the dynamics towards a neighborhood of a different sector of  $\mathcal{K}$ . Also, outside the regime  $-1 < k(x) < 2$ , spikes of higher order may form along exceptional timelines, through choice of special initial conditions.

In recent numerical work, Garfinkle and Weaver [21] investigated spikes with  $k(x)$  initially outside the regime  $-1 < k(x) < 2$  and reported that they generally disappear in the process of evolution. It has been suggested by Lim [32] that so-called *spike transition orbits* could provide an explanation for this phenomenon. Unfortunately, no analytic approximations are available to date and further work is needed. Nevertheless, numerical experiments so far indicate that the limit (5.8) does hold for timelines with nonspecial initial conditions [32].

According to a conjecture by Uggla *et al* [38, §4.1], the exceptional dynamical behavior towards the singularity along those timelines where either false or true spikes form does not disturb the overall asymptotically silent nature of the dynamics, as in the (here) asymptotic limit  $t \rightarrow +\infty$  any spatial inhomogeneity



associated with the formation of spikes is pushed beyond the particle horizon of every individual timeline, and so cannot be perceived by observers traveling along the timelines.<sup>13</sup>

The present consideration provides a natural basis for classifying spikes as “low velocity” or “high velocity”, according to Rendall and Weaver [34] and Garfinkle and Weaver [21]. By Eqs. (5.9),

- (1) “low velocity” arises (a) for false spikes when  $0 = \hat{\Sigma}_\times$  and  $-1 < k(x) < 0$ , (b) for true spikes when  $0 = \hat{N}_-$  and  $1 < k(x) < 2$ ,
- (2) “high velocity” arises (a) for false spikes when  $0 = \hat{\Sigma}_\times = \partial_x \hat{\Sigma}_\times$  and  $k(x) < -1$ , (b) for true spikes when  $0 = \hat{N}_- = \partial_x \hat{N}_-$  and  $k(x) \geq 2$ .

Due to the strong constraints that need to be satisfied, (persistent) high velocity spikes are nongeneric.

For fixed  $x$ , the definition of the function  $k(x)$  given in Eq. (5.5) provides an alternative parametrization of the Kasner circle. This is of some interest since, according to Kichenassamy and Rendall [29, p. 1341], the asymptotic hyperbolic velocity  $\hat{v}(x)$  defined in Eq. (5.1) and  $k(x)$  are related by

$$\hat{v}(x) = |k(x)| .$$

In this parametrization of  $\mathcal{K}$ , the special points  $Q_\alpha$  and  $T_\alpha$  correspond to the values

$$\begin{aligned} Q_1 : k = 0 , & & T_3 : k = -1 , \\ Q_2 : k = -3 , & & T_1 : k = \infty , \\ Q_3 : k = 3 , & & T_2 : k = 1 . \end{aligned}$$

In addition, the value  $k = 2$  corresponds to  $(\Sigma_+, \Sigma_-) = (-1/7, -4\sqrt{3}/7)$ . The marked points on the Kasner circles in Figs. 14 and 15 are (from the left) the points with  $k = \infty, 2, 1, 0$ .

Returning to the discussion of the asymptotic dynamics as  $t \rightarrow +\infty$ , as briefly mentioned above our numerical simulations suggest that the product between the “ $\times$ -polarization variables”  $(\Sigma_\times, N_-)$ , which span the unstable directions on the unstable sectors of the Kasner circle (and are also responsible for the spike formation process), satisfies the limit

$$\lim_{t \rightarrow +\infty} N_- \Sigma_\times = 0 . \tag{5.10}$$

This behavior, a special case of Eq. (101) in Ref. [38], is further reflected in the linear solutions given in Eqs. (5.7), which, for  $t \rightarrow +\infty$ , yield exponentially fast decay of  $N_- \Sigma_\times$  as  $e^{-t}$ . In the same regime,  $N_\times \Sigma_-$  decays exponentially fast as  $te^{-t}$ , so that, by Eq. (3.12c),  $\dot{U}$  decays as  $te^{-t}$ , and so does  $r$  by Eq. (3.12a). The linear analysis thus strengthens the emerging picture of the dynamical behavior along typical timelines of Gowdy vacuum spacetimes in the approach to the singularity.

---

<sup>13</sup>In unpublished work, Woei Chet Lim and John Wainwright have constructed an explicit exact solution with a true spike for which the conjecture has been shown to be analytically true. Moreover, unpublished numerical work by Lim suggests that for Gowdy vacuum spacetimes this is true in general. Thus, there exists evidence for asymptotic silence to hold even when spatial derivatives blow up due to the formation of spikes.

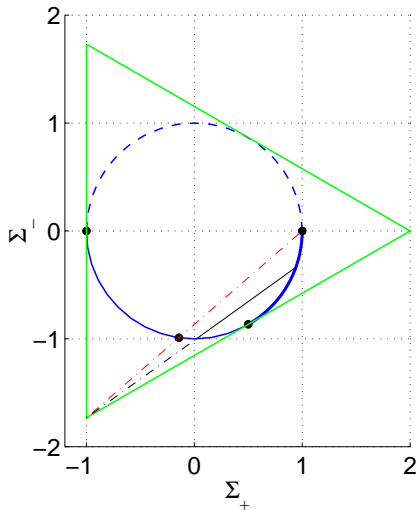


FIG. 16. Curvature transition orbit of Bianchi Type-II.

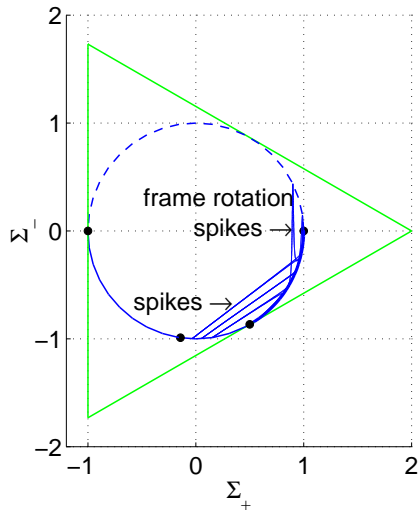


FIG. 17. Snapshot of the solution at  $t = 12$ , projected into the  $(\Sigma_+ \Sigma_-)$ -plane. Frame transition and curvature transition orbits are indicated.

Asymptotic silence holds for Gowdy vacuum spacetimes since  $E_1^1 \rightarrow 0$  uniformly as  $t \rightarrow +\infty$ ; see Eq. (5.2). Our numerical calculations indicate that  $N_- \Sigma_\times \rightarrow 0$  and  $N_\times \Sigma_- \rightarrow 0$  uniformly (see Fig. 13) so that  $\dot{U} \rightarrow 0$  and  $r \rightarrow 0$  uniformly as  $t \rightarrow +\infty$ . It follows that the dynamics of Gowdy vacuum spacetimes are increasingly well approximated by the dynamics on the silent boundary. The latter lead to a characteristic interplay between  $\Sigma_\times$ -induced frame transitions and  $N_-$ -induced curvature transitions on the Kasner circle associated with each timeline; they give rise to a *finite sequence* of transitions from one unstable position on  $\mathcal{K}$  to another one, until, eventually, a position on the stable arc  $(T_2 Q_1)$  of  $\mathcal{K}$  is reached. This behavior is shown clearly in Figs. 15–17. The interplay between the frame transitions and the curvature transitions provides a simple mechanism for forcing the function  $k(x)$  to satisfy

$$|k(x)| < 1 ,$$

along typical timelines. Understanding the reduction of the value of the hyperbolic velocity  $v(t, x)$  to the regime  $\hat{v}(x) = |k(x)| < 1$  along typical timelines in the evolution of Gowdy vacuum spacetimes towards the singularity is stated as an open problem by Kichenassamy and Rendall [29, p. 1341].

**5.3. Behavior of Weyl curvature.** We now evaluate the asymptotic behavior of the Hubble-normalized electric and magnetic Weyl curvature (relative to  $e_0$ ) for Gowdy vacuum spacetimes in the so-called “low velocity” regime  $0 < k(x) <$

1, i.e., for typical timelines with the dynamics in a small neighborhood of the stable arc( $T_2Q_1$ )  $\subset \mathcal{K}$ . Substituting the linear solutions (5.6) and (5.7) into the Weyl curvature formulae given in App. A.1, we obtain

$$\mathcal{E}_+ = \frac{6[1 - k^2(x)]}{[3 + k^2(x)]^2} + \mathcal{O}(e^{-t}) + \mathcal{O}(e^{-2[1-k(x)]t}) + \mathcal{O}(e^{-2k(x)t}) , \quad (5.11a)$$

$$\mathcal{H}_+ = \mathcal{O}(e^{-[1-k(x)]t}) + \mathcal{O}(te^{-[1+k(x)]t}) , \quad (5.11b)$$

$$\mathcal{E}_- = \frac{2\sqrt{3}k(x)[1 - k^2(x)]}{[3 + k^2(x)]^2} + \mathcal{O}(e^{-t}) + \mathcal{O}(e^{-2[1-k(x)]t}) , \quad (5.11c)$$

$$\mathcal{H}_\times = \mathcal{O}(te^{-t}) , \quad (5.11d)$$

$$\mathcal{E}_\times = \mathcal{O}(e^{-k(x)t}) , \quad (5.11e)$$

$$\mathcal{H}_- = \mathcal{O}(e^{-[1-k(x)]t}) + \mathcal{O}(te^{-[1+k(x)]t}) . \quad (5.11f)$$

In the limit  $t \rightarrow +\infty$ , the magnetic Weyl curvature decays exponentially fast, so that for the electric Weyl curvature the Kasner limit is attained pointwise.

## 6. CONCLUDING REMARKS

In  $G_0$  cosmology, as in the Gowdy case, the evolution equations on the silent boundary for the Hubble-normalized dimensionless coordinate scalars (i.e., all variables except the frame variables  $E_\alpha^i$ ), given in Ref. [38, §2], are identical to those for the same quantities when describing SSS and SH models. The reason for this is the following. Dimensionless scalars of SSS and SH models are by definition purely time-dependent (in symmetry adapted coordinates), and thus the spatial frame derivatives that appear in the equations for the Hubble-normalized dimensionless coordinate scalars drop out, which leads to a decoupling of the frame variables  $E_\alpha^i$ . The resulting system of equations is clearly the same as that obtained by setting the spatial frame derivatives to zero, as done on the silent boundary.

In the identification of the equations on the silent boundary with the SSS and SH equations, the normalization is essential; it is only when dealing with scale-invariant dimensionless variables that one obtains a direct correspondence. As discussed by Eardley [15], a SSS geometry is related to a SH geometry by a spatially dependent conformal transformation; by introducing dimensionless variables the conformal factor drops out and one obtains SH quantities. The silent boundary of the  $G_0$  state space consists of a union of the most general SSS and SH models, notably SH Bianchi Type–VIII and Type–IX models and self-similar models of class D (see Ref. [15, §3] for notation).<sup>14</sup> To obtain a detailed proof of the SSS/SH silent boundary correspondence, one can start with the SSS and SH symmetry adapted metric representation given by Eardley [15, §3],

---

<sup>14</sup>The joint SSS and SH character of the silent boundary is in accordance with the attempt in Ref. [38] to heuristically explain the dynamical importance of the silent boundary: ultra-strong gravitational fields associated with typical spacelike singularities collapse the local null cones, which thus prevents information propagation yielding local dynamics. SSS spacetimes are conformally SH, and thus also SSS dynamics are purely local. Moreover, the “pathological” spatial properties of SSS spacetimes are irrelevant; only their temporal properties are of interest in the approach to a spacelike singularity.

and then derive the correspondence through a direct comparison between the SSS/SH equations and those on the silent boundary.

Gowdy vacuum spacetimes form an invariant set of the general  $G_0$  state space. The intersection of this invariant set with the SSS and SH subsets in turn yields an invariant subset which is described by the equations on the silent boundary of the Gowdy state space.

### 6.1. AVTD and BKL from the point of view of the silent boundary.

Discussions of AVTD behavior near spacetime singularities and of the BKL conjecture on oscillatory behavior of vacuum dominated singularities have often been associated with claims that the asymptotic dynamical behavior in the direction of the singularity of spatially inhomogeneous spacetimes is locally like that of SH models. Indeed, BKL take as a starting point for their analysis explicit SH solutions. They replace the integration constants by spatially dependent functions and perform a perturbation analysis in the asymptotic regime around the resulting ansatz. The dynamical systems approach offers some justification for this procedure.<sup>15</sup>

Due to the SSS/SH silent boundary correspondence, the reduced system of equations on the silent boundary leads to the same solutions for the Hubble-normalized coordinate scalars in both cases. However, in contrast to the true SSS/SH cases, the constants of integration become spatially dependent functions on the silent boundary. Then, in the true SSS/SH cases, the metric is obtained in a subsequent step, by integrating the decoupled system of equations for the frame variables  $E_\alpha^i$ . However, the silent boundary (where  $0 = E_\alpha^i$ ) is unphysical, since it corresponds to a degenerate metric. In order to obtain an expression for the metric which is valid in the asymptotic regime, one is forced to go into the physical *interior part* of the state space where the  $E_\alpha^i$  are nonzero. By perturbing around  $0 = E_\alpha^i$ , starting from a seed solution to the reduced system of equations on the silent boundary, approximate solutions to the full system can be constructed. To lowest order, the asymptotic approximation so obtained is identical to the corresponding true SSS/SH solution, but with integration constants replaced by spatially dependent functions which in turn are restricted by the Codacci constraint.

In terms of the discussion in this paper, the AVTD leading order solution for Gowdy vacuum spacetimes is produced by the above procedure using a seed solution taking values in the Kasner subset on the silent boundary (note that VTD is associated with the entire silent Kasner subset, while AVTD is associated only with the stable part(s) of the Kasner circle). Indeed, the linearization at the stable arc of the Kasner circle yields the starting point for the analysis of Kichenassamy and Rendall [29]. Similarly, BKL in their analysis consider seed data in the Taub subset (vacuum Bianchi Type-II) on the silent boundary, in addition to the Kasner subset. Thus, the AVTD and BKL analysis has

---

<sup>15</sup>An alternative point of view on the oscillatory approach to the singularity is provided by the method of consistent potentials (see Ref. [7] for a discussion of the  $T^2$ -symmetric case). Further, Thibault Damour, Marc Henneaux and collaborators have recently developed a picture of the asymptotic behavior of stringy gravity in  $D = 10$  spacetime dimensions, which leads to consideration of hyperbolic billiards (see Refs. [13] and [14], and references therein).

considered only part of the past attractor conjectured in Ref. [38], while on the contrary, the results in the present paper indicate that it is essential to consider the *entire* silent boundary in order to understand the approach towards the singularity.

**6.2. Gowdy case.** We conclude by discussing the picture that emerges in the Gowdy case. In view of the non-oscillatory nature of the system of equations on the silent boundary, we expect Gowdy vacuum spacetimes to have a non-oscillatory singularity in the sense that  $\lim_{t \rightarrow +\infty} \mathbf{X}(t, x) = \hat{\mathbf{X}}(x)$  exists, and that  $\hat{\mathbf{X}}$  takes values only on the Kasner circle  $\mathcal{K}$  on the silent boundary. Moreover, the local stability of the arc  $(T_2Q_1) \subset \mathcal{K}$  suggests that it is a local attractor, i.e.,

$$\mathcal{A} = \text{arc}(T_2Q_1) \subset \mathcal{K} = \mathcal{A}_{\text{Gowdy}}^- .$$

This was indeed proved by Ringström [36, 37] and Chae and Chruściel [9]: if  $\mathbf{X}(t, x)$  is sufficiently close to  $\mathcal{A}$ , in a suitable sense, then  $\lim_{t \rightarrow +\infty} \mathbf{X}(t, x) = \hat{\mathbf{X}}(x)$ , with  $\hat{\mathbf{X}}(x): S^1 \rightarrow \mathcal{A}$  a continuous map, and the limit is in the uniform topology. Chae and Chruściel [9] have also proved that for any Gowdy vacuum spacetime with smooth initial data, there is an open and dense subset  $O \subset S^1$ , such that for  $x \in O$ ,  $\lim_{t \rightarrow +\infty} \mathbf{X}(t, x) = \hat{\mathbf{X}}(x)$ ,  $\hat{\mathbf{X}}(x) \in \mathcal{A}$ , and  $\hat{\mathbf{X}}$  is smooth at  $x$ . Furthermore, they showed that, for any closed  $F \subset S^1$  with empty interior, a solution could be constructed with (false) spikes on  $F$ . By applying Gowdy-to-Ernst transformations, these can presumably be turned into true spikes with high velocity. This shows that the detailed asymptotic behavior of Gowdy vacuum spacetimes can be quite complicated. A very useful further step in the mathematical analysis of Gowdy vacuum spacetimes would be to prove that it is always the case that  $\lim_{t \rightarrow +\infty} (\Sigma_- N_\times)^2 + (\Sigma_\times N_-)^2 = 0$ . A limit of this kind reflects that in the asymptotic regime the propagation of gravitational waves (represented by the “+ -polarization variables”  $(\Sigma_-, N_\times)$  and the “ $\times$ -polarization variables”  $(\Sigma_\times, N_-)$ , respectively) becomes dynamically insignificant.

If one considers *generic* smooth initial data, the picture should simplify considerably. For example, since a generic smooth function has at most a finite number of zeros on a finite interval, and true spikes correspond to zeros of  $Q_{,x}$ , one expects that generic solutions have at most a finite number of true spikes. An analogous argument indicates that a generic solution has at most a finite number of (true or false) spikes. High velocity spikes are expected to be nongeneric since they correspond to higher order zeros of  $Q_{,x}$ . Therefore, one expects that a generic solution will have a finite number of true spikes, all with velocity in the interval  $(1, 2)$ .

Due to the existence of spikes for general Gowdy vacuum spacetimes,  $\mathcal{A}$  *cannot* be a global attractor. For a Gowdy solution with spikes,

$$\lim_{t \rightarrow +\infty} \sup_{x \in S^1} d(\mathbf{X}(t, x), \mathcal{K}) \neq 0 ,$$

even though we expect that the *pointwise* limit is a map to  $\mathcal{K}$ . This makes it clear that the notions of “asymptotic state” and “attractor” depend, in the spatially inhomogenous case, on the choice of topology.

The numerical work in this paper indicates that the variety

$$\mathcal{U} = \{\Sigma_- N_\times = \Sigma_\times N_- = 0\}$$

is the *uniform* attractor for Gowdy vacuum spacetimes in the sense that

$$\lim_{t \rightarrow +\infty} \sup_{x \in S^1} d(\mathbf{X}(t, x), \mathcal{U}) = 0 .$$

As seen from the discussion in Subsec. 5.2, the silent boundary dynamics on  $\mathcal{U}$  explain the major evolutionary features along typical Gowdy timelines.

The state space framework for spatially inhomogeneous cosmology based on the dynamical systems approach offers a common ground where many scattered results and conjectures may be collected and put into a broader context. For example, earlier claims and results as regards SH models can now be regarded as results determined by the structure of the silent boundary of the Hubble-normalized state space. This pertains, e.g., to work by BKL, conjectures and proofs in WE, and proofs by Ringström. The latter showed in Ref. [35] that the Bianchi Type-II variety is a past attractor for nontilted SH perfect fluid models of Bianchi Type-IX.<sup>16</sup>

Finally, earlier results, and the results in this paper, suggest that the silent boundary, perturbations thereof, and the formation of spikes, in a  $G_2$  as well as in a  $G_0$  context, are worthy areas of exploration, and are likely to offer exciting hunting grounds in the coming years.

#### ACKNOWLEDGMENTS

We thank Woei Chet Lim, John Wainwright, and Piotr Chruściel for helpful comments. Further, we are grateful to Mattias Sandberg for his work during the early stages of this project.

#### APPENDIX A. HUBBLE-NORMALIZED WEYL CURVATURE

**A.1. Variables.** The Hubble-normalized electric and magnetic Weyl curvatures (relative to  $e_0$ ) for Gowdy vacuum spacetimes can be easily obtained by specializing the relations given in Ref. [18]. The “+”, “−” and “ $\times$ ” variables

---

<sup>16</sup>This attractor organizes the past asymptotic dynamics and provides an explanation for the Kasner-billiard-like behavior of nontilted SH models of Bianchi Type-IX in the approach to the singularity. The same variety is expected to be the past attractor for nontilted SH models of Bianchi Type-VIII. A candidate attractor variety has been identified for nontilted SH perfect fluid models of Bianchi Type-VI\*<sub>-1/9</sub> by Hewitt *et al* [25]. This is the only nontilted SH model in class B that exhibits oscillatory dynamical behavior into the past.

are defined analogous to the shear rate variables in Eqs. (2.13).

$$\mathcal{E}_+ = \frac{2}{3}(N_\times^2 + N_-^2) + \frac{1}{3}(1 + \Sigma_+) \Sigma_+ - \frac{1}{3}(\Sigma_-^2 + \Sigma_\times^2), \quad (\text{A.1a})$$

$$\mathcal{H}_+ = -N_- \Sigma_- - N_\times \Sigma_\times, \quad (\text{A.1b})$$

$$\mathcal{E}_- = \frac{1}{3}(E_1^1 \partial_x - r) N_\times + \frac{2}{\sqrt{3}} N_-^2 + \frac{1}{3}(1 - 2\Sigma_+) \Sigma_-, \quad (\text{A.1c})$$

$$\mathcal{H}_\times = \frac{1}{3}(E_1^1 \partial_x - r) \Sigma_- - \frac{2}{\sqrt{3}} N_- \Sigma_\times - N_\times \Sigma_+, \quad (\text{A.1d})$$

$$\mathcal{E}_\times = -\frac{1}{3}(E_1^1 \partial_x - r) N_- + \frac{2}{\sqrt{3}} N_\times N_- + \frac{1}{3}(1 - 2\Sigma_+) \Sigma_\times, \quad (\text{A.1e})$$

$$\mathcal{H}_- = -\frac{1}{3}(E_1^1 \partial_x - r) \Sigma_\times - \frac{2}{\sqrt{3}} N_- \Sigma_- - N_- \Sigma_+. \quad (\text{A.1f})$$

### A.2. Spatial scalars.

$$\mathcal{E}_{\alpha\beta} \mathcal{E}^{\alpha\beta} = 6(\mathcal{E}_+^2 + \mathcal{E}_-^2 + \mathcal{E}_\times^2), \quad (\text{A.2a})$$

$$\mathcal{H}_{\alpha\beta} \mathcal{H}^{\alpha\beta} = 6(\mathcal{H}_+^2 + \mathcal{H}_-^2 + \mathcal{H}_\times^2), \quad (\text{A.2b})$$

$$\mathcal{E}_{\alpha\beta} \mathcal{H}^{\alpha\beta} = 6(\mathcal{E}_+ \mathcal{H}_+ + \mathcal{E}_- \mathcal{H}_- + \mathcal{E}_\times \mathcal{H}_\times), \quad (\text{A.2c})$$

$$\mathcal{E}_\alpha^\beta \mathcal{E}_\beta^\gamma \mathcal{E}_\gamma^\alpha = -6\mathcal{E}_+ (\mathcal{E}_+^2 - 3\mathcal{E}_-^2 - 3\mathcal{E}_\times^2), \quad (\text{A.2d})$$

$$\mathcal{H}_\alpha^\beta \mathcal{H}_\beta^\gamma \mathcal{H}_\gamma^\alpha = -6\mathcal{H}_+ (\mathcal{H}_+^2 - 3\mathcal{H}_-^2 - 3\mathcal{H}_\times^2), \quad (\text{A.2e})$$

$$\mathcal{E}_\alpha^\beta \mathcal{H}_\beta^\gamma \mathcal{H}_\gamma^\alpha = -6[\mathcal{E}_+ (\mathcal{H}_+^2 - \mathcal{H}_-^2 - \mathcal{H}_\times^2) - 2\mathcal{E}_- \mathcal{H}_+ \mathcal{H}_- - 2\mathcal{E}_\times \mathcal{H}_+ \mathcal{H}_\times], \quad (\text{A.2f})$$

$$\mathcal{H}_\alpha^\beta \mathcal{E}_\beta^\gamma \mathcal{E}_\gamma^\alpha = -6[\mathcal{H}_+ (\mathcal{E}_+^2 - \mathcal{E}_-^2 - \mathcal{E}_\times^2) - 2\mathcal{H}_- \mathcal{E}_+ \mathcal{E}_- - 2\mathcal{H}_\times \mathcal{E}_+ \mathcal{E}_\times]. \quad (\text{A.2g})$$

### A.3. Spacetime scalars.

$$\mathcal{I}_1 = 8(\mathcal{E}_{\alpha\beta} \mathcal{E}^{\alpha\beta} - \mathcal{H}_{\alpha\beta} \mathcal{H}^{\alpha\beta}), \quad (\text{A.3a})$$

$$\mathcal{I}_2 = -16\mathcal{E}_{\alpha\beta} \mathcal{H}^{\alpha\beta}, \quad (\text{A.3b})$$

$$\mathcal{I}_3 = -16(\mathcal{E}_\alpha^\beta \mathcal{E}_\beta^\gamma \mathcal{E}_\gamma^\alpha - 3\mathcal{E}_\alpha^\beta \mathcal{H}_\beta^\gamma \mathcal{H}_\gamma^\alpha), \quad (\text{A.3c})$$

$$\mathcal{I}_4 = 16(\mathcal{H}_\alpha^\beta \mathcal{H}_\beta^\gamma \mathcal{H}_\gamma^\alpha - 3\mathcal{H}_\alpha^\beta \mathcal{E}_\beta^\gamma \mathcal{E}_\gamma^\alpha). \quad (\text{A.3d})$$

$\mathcal{I}_1$  is the Hubble-normalized Kretschmann scalar.

## REFERENCES

1. Guido Beck, *Zur Theorie binärer Gravitationsfelder*, Z. Phys. **33** (1925), 713–728.
2. Vladimir A. Belinskii, Isaac M. Khalatnikov, and Evgeny M. Lifshitz, *Oscillatory approach to a singular point in the relativistic cosmology*, Adv. Phys. **19** (1970), 525–573.
3. ———, *A general solution of the Einstein equations with a time singularity*, Adv. Phys. **31** (1982), 639–667.
4. Beverly K. Berger, *Approach to the singularity in spatially inhomogeneous cosmologies*, Differential equations and mathematical physics (Birmingham, AL, 1999), AMS/IP Stud. Adv. Math., vol. 16, Amer. Math. Soc., Providence, RI, 2000, pp. 27–40.
5. Beverly K. Berger and David Garfinkle, *Phenomenology of the Gowdy universe on  $T^3 \times R$* , Phys. Rev. D **57** (1998), 4767–4777.

6. Beverly K. Berger, David Garfinkle, James Isenberg, Vincent Moncrief, and Marsha Weaver, *The singularity in generic gravitational collapse is spacelike, local and oscillatory*, Modern Phys. Lett. A **13** (1998), no. 19, 1565–1573.
7. Beverly K. Berger, James Isenberg, and Marsha Weaver, *Oscillatory approach to the singularity in vacuum spacetimes with  $T^2$  isometry*, Phys. Rev. D **64** (2001), no. 8, 084006–20.
8. Beverly K. Berger and Vincent Moncrief, *Numerical investigation of cosmological singularities*, Phys. Rev. D **48** (1993), no. 10, 4676–4687.
9. Myeongju Chae and Piotr T. Chruściel, *On the dynamics of Gowdy space-times*, gr-qc/0305029, 2003.
10. Piotr T. Chruściel, *On space-times with  $U(1) \times U(1)$  symmetric compact Cauchy surfaces*, Ann. Physics (N.Y.) **202** (1990), no. 1, 100–150.
11. Piotr T. Chruściel, James Isenberg, and Vincent Moncrief, *Strong cosmic censorship in polarised Gowdy spacetimes*, Classical Quantum Gravity **7** (1990), no. 10, 1671–1680.
12. C. Barry Collins, *More qualitative cosmology*, Commun. Math. Phys. **23** (1971), 137–158.
13. Thibault Damour and Marc Henneaux,  *$E_{10}$ ,  $BE_{10}$  and arithmetical chaos in superstring cosmology*, Phys. Rev. Lett. **86** (2001), no. 21, 4749–4752.
14. Thibault Damour, Marc Henneaux, and Hermann Nicolai, *Cosmological billiards*, Classical Quantum Gravity **20** (2003), no. 9, R145–R200.
15. Douglas M. Eardley, *Self-similar spacetimes: geometry and dynamics*, Commun. Math. Phys. **37** (1974), 287–309.
16. Albert Einstein and Nathan Rosen, *On gravitational waves*, J. Franklin Inst. **223** (1937), 43–54.
17. George F. R. Ellis and Malcolm A. H. MacCallum, *A class of homogeneous cosmological models*, Commun. Math. Phys. **12** (1969), 108–141.
18. Henk van Elst, *Hubble-normalised orthonormal frame equations for perfect fluid cosmologies in component form*, URL: [www.maths.qmul.ac.uk/~hve/research.html](http://www.maths.qmul.ac.uk/~hve/research.html), 2002.
19. Henk van Elst and Claes Uggla, *General relativistic 1+3 orthonormal frame approach*, Classical Quantum Gravity **14** (1997), no. 9, 2673–2695.
20. Henk van Elst, Claes Uggla, and John Wainwright, *Dynamical systems approach to  $G_2$  cosmology*, Classical Quantum Gravity **19** (2002), no. 1, 51–82.
21. David Garfinkle and Marsha Weaver, *High velocity spikes in Gowdy spacetimes*, Phys. Rev. D **67** (2003), no. 12, 124009–5.
22. Robert H. Gowdy, *Gravitational waves in closed universes*, Phys. Rev. Lett. **27** (1971), no. 12, 826–829.
23. ———, *Vacuum spacetimes and compact invariant hyperspaces: Topologies and boundary conditions*, Ann. Physics (N.Y.) **83** (1974), 203–241.
24. Boro Grubišić and Vincent Moncrief, *Asymptotic behavior of the  $T^3 \times R$  Gowdy spacetimes*, Phys. Rev. D **47** (1993), no. 6, 2371–2382.
25. Conrad G. Hewitt, Joshua T. Horwood, and John Wainwright, *Asymptotic dynamics of the exceptional Bianchi cosmologies*, Classical Quantum Gravity **20** (2003), no. 9, 1743–1756.
26. Conrad G. Hewitt and John Wainwright, *Orthogonally transitive  $G_2$  cosmologies*, Classical Quantum Gravity **7** (1990), no. 12, 2295–2316.
27. James Isenberg, Martin Jackson, and Vincent Moncrief, *Evolution of the Bel–Robinson energy in Gowdy  $T^3 \times R$  space-times*, J. Math. Phys. **31** (1990), no. 2, 517–519.
28. James Isenberg and Vincent Moncrief, *Asymptotic behavior of the gravitational field and the nature of singularities in Gowdy spacetimes*, Ann. Physics (N.Y.) **199** (1990), no. 1, 84–122.
29. Satyanad Kichenassamy and Alan D. Rendall, *Analytic description of singularities in Gowdy spacetimes*, Classical Quantum Gravity **15** (1998), no. 5, 1339–1355.
30. Andrew R. King and George F. R. Ellis, *Tilted homogeneous cosmological models*, Commun. Math. Phys. **31** (1973), 209–242.
31. Randall J. LeVeque, *Finite Volume Methods for Hyperbolic Problems*, Cambridge University Press, Cambridge, 2002.
32. Woei Chet Lim, private communication, 2003.



33. Vincent Moncrief, *Global properties of Gowdy spacetimes with  $T^3 \times R$  topology*, Ann. Physics (N.Y.) **132** (1981), no. 1, 87–107.
34. Alan D. Rendall and Marsha Weaver, *Manufacture of Gowdy spacetimes with spikes*, Classical Quantum Gravity **18** (2001), no. 15, 2959–2975.
35. Hans Ringström, *The Bianchi IX attractor*, Ann. Henri Poincaré **2** (2001), no. 3, 405–500.
36. ———, *On Gowdy vacuum spacetimes*, gr-qc/0204044, 2002.
37. ———, *Asymptotic expansions close to the singularity in Gowdy spacetimes*, gr-qc/0303051, 2003.
38. Claes Uggla, Henk van Elst, John Wainwright, and George F. R. Ellis, *The past attractor in inhomogeneous cosmology*, gr-qc/0304002, 2003.
39. John Wainwright, *A classification scheme for non-rotating inhomogeneous cosmologies*, J. Phys. A: Math. Gen. **12** (1979), no. 11, 2015–2029.
40. John Wainwright and George F. R. Ellis (editors), *Dynamical Systems in Cosmology*, Cambridge University Press, Cambridge, 1997.
41. John Wainwright and Lucas Hsu, *A dynamical systems approach to Bianchi cosmologies: orthogonal models of class A*, Classical Quantum Gravity **6** (1989), no. 10, 1409–1431.

DEPARTMENT OF MATHEMATICS, UNIVERSITY OF MIAMI, CORAL GABLES, FL 33124, USA

*E-mail address:* `larsa@math.kth.se`

ASTRONOMY UNIT, QUEEN MARY, UNIVERSITY OF LONDON, MILE END ROAD, LONDON E1 4NS, UNITED KINGDOM

*E-mail address:* `H.van.Elst@qmul.ac.uk`

DEPARTMENT OF PHYSICS, UNIVERSITY OF KARLSTAD, S-651 88 KARLSTAD, SWEDEN

*E-mail address:* `Claes.Uggla@kau.se`